AD-A112 918 BATTELLE COLUMBUS LABS OH F/G 13/5
TREND INSPECTION STATION FOR PRINTED CIRCUIT BOARD SOLDER JOINT--ETC(U)
SEP 81 T S SMILLIDAY, F B STULEN F09603-80-G-0420
UNCLASSIFIED NL

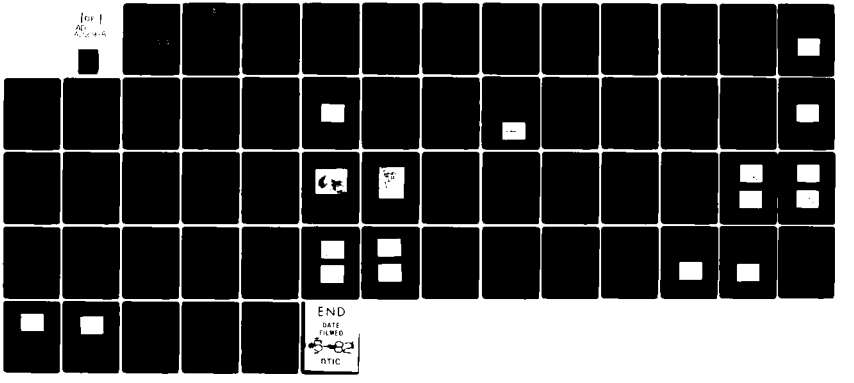

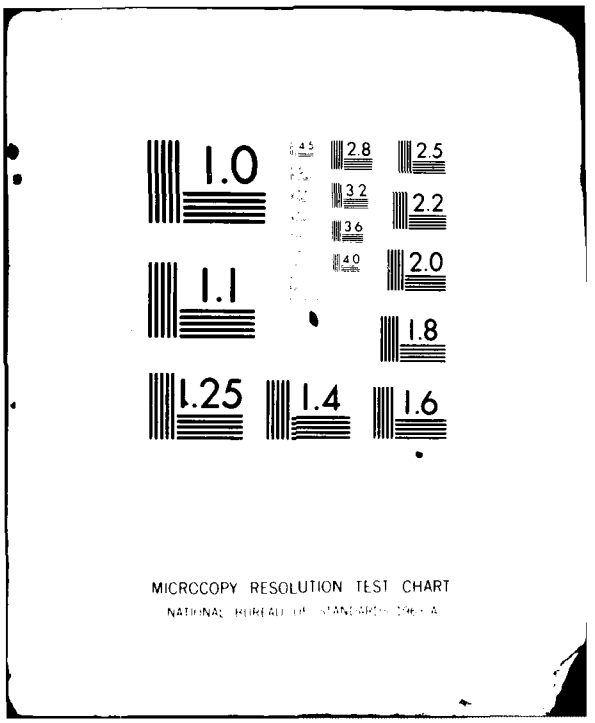
1.0
1.1
1.25
1.4
1.6
1.8
2.0
2.2
2.5
2.8
3.2
3.6
4.0
4.5
MICRCCOPY RESOLUTION TEST CHART

PHOTOGRAPH THIS SHEET

AD-A112918

DTIC ACCESSION NUMBER

LEVEL

INVENTORY

Final Engineering Rept. Phase 2.2
29 Sept. 81

DOCUMENT IDENTIFICATION

Contract F09603-80-G-0420

DISTRIBUTION STATEMENT A
Approved for public release;
Distribution Unlimited

DISTRIBUTION STATEMENT

ACCESSION FOR	
NTIS	GRA&I
DTIC	TAB
UNANNOUNCED	
JUSTIFICATION	
BY	Per Ltr. on file
DISTRIBUTION / AVAILABILITY CODES	
DIST	AVAIL AND/OR SPECIAL
A	

DISTRIBUTION STAMP

DTIC
ELECTE
S APR 2 1982 D
D

DATE ACCESSIONED

DATE RECEIVED IN DTIC

PHOTOGRAPH THIS SHEET AND RETURN TO DTIC-DDA-2

DTIC FORM OCT 79 70A

DOCUMENT PROCESSING SHEET

Battelle
Columbus Laboratories

AD A113 969

Report

FINAL ENGINEERING REPORT

on

PHASE 2.2,
TREND INSPECTION STATION FOR
PRINTED CIRCUIT BOARD SOLDER JOINTS,
ULTRASONIC SUBSYSTEM

to

SACRAMENTO AIR LOGISTICS CENTER

September 29, 1981

by

T. S. Shilliday, F. B. Stulen,
T. L. Fletcher, and D. Becker

BOA F09603-80-G-04
Delivery Order No. S401

BATTELLE
Columbus Laboratories
505 King Avenue
Columbus, Ohio 43201

TABLE OF CONTENTS

LIST OF TABLES

Page

LIST OF FIGURES

Figure 1

Page

FINAL ENGINEERING REPORT

on

PHASE 2.2,
TREND INSPECTION STATION FOR PRINTED CIRCUIT
BOARD SOLDER JOINTS, ULTRASONIC SUBSYSTEM

to

SACRAMENTO AIR LOGISTICS CENTER

from

BATTELLE
Columbus Laboratories

by

T. S. Shilliday, F. B. Stulen, T. L. Fletcher, and D. Becker

INTRODUCTION AND SUMMARY

This is the Final Engineering Report on Phase 2.2 work on the ultrasonic subsystem for the trend inspection station for printed circuit board solder joints. The report discusses activities during this contract period in six major areas.

Probe assemblies have been refined by redesigning both receiver and transmitter to permit closer spacing of these probes for inspection of small joints. In addition, transmitter design has resulted in a new style probe.

Based in part on the characteristics of ultrasonic spectra of the solder joint types of interest, and in part on the mental processes used in visual evaluation of joint spectra to make a judgment on joint quality, several algorithms have been investigated for computerizing the decision making process. A simple but effective algorithm has been devised for use with the latest probe set in inspecting good lap solder joints and those with heel cracks.

A probe manipulator for the pilot model of the ultrasonic subsystem was designed and constructed during this contract period. It was used in some of the later experimentation in this period directed to defining performance capability.

It is a goal of the Air Force to have an inspection system which will incorrectly identify as cracked no more than 0.5 percent of the good joints inspected. An experiment was designed and carried out to demonstrate how effectively the existing system would perform in relation to this goal. The results indicated that the goal has been achieved.

Essentially all of the work done thus far in the development of the ultrasonic inspection subsystem has been done on ribbon leads on integrated circuit flat packs. As an initial step toward extending capability of the inspection system to accommodate all types of joints, some work was done during this contract period on lap joints in round resistor leads 25 mils in diameter. In a sampling of good joints and joints with heel cracks, the automated system correctly identified all of the good joints and about two-thirds of the cracked joints. These results permit an optimistic outlook toward the system being able to work effectively on joints having a variety of conformations.

Finally, an investigation was made of the risk of inadvertently damaging, with the applied ultrasonic energy, joints under inspection or the electronic components associated with them. At power levels at least 100 times those normally used for inspection and exposure periods of the order of 100 times longer than those used for inspection of a joint, no damage to operating integrated circuits was observed. It therefore seems reasonable to conclude that the risk of introducing damage as a result of the ultrasonic energy at the level being used for inspection is quite remote.

PROBE ASSEMBLY REFINEMENT

Three probes were designed, constructed and evaluated during this contract period. One was a receiver similar to the previous design. The other two were transmitters; one was designed to use a different mode of vibration than the past transmitters, and the other was a simplified design of the style of transmitter used in the previous phases of this project.

A major design criteria is that the transmitters and receivers have parallel vertical sides so that the interprobe distance can be as small as possible. This design allows even very short joints to be tested. The following describes the design, construction, and general performance of the probes built.

Receiver

The receiver is designed as a wedge-shaped, half-wave, longitudinal receiver. This has the form shown in Figure 1. The dimensions of the end faces of the horn are selected from geometrical considerations. The dimensions of the tip are 0.05 inch by 0.005 inch. This is a knife-edge contact where the width is great enough to span the width of most all lap solder joints. The other end is 0.125 inch by 0.125 inch to keep the overall dimensions small; furthermore, 1/8 inch square stock is readily available. The width and the thickness can both be expressed as a linear function of position. Therefore the cross sectional area, S, of any plane can be described by a quadratic equation:

$$S = ax^2 + bx + c \tag{1}$$

where a, b, and c are constant coefficients and x is the position. If the coefficients b and c are zero so that the area is proportional to the square of position, then the differential equation of motion can be solved in closed form. The general solution for longitudinal vibrations in a horn is given by

$$\frac{d^2Y}{dx^2} + \left[\frac{dS/dx}{S}\right]\frac{dY}{dx} + k^2Y = 0 \tag{2}$$

where Y is the amplitude of vibration and k is the wave number. When $S = ax^2$, the equation reduces to

$$\frac{d^2Y}{dx^2} + \frac{2}{x}\frac{dY}{dx} + k^2Y = 0 \tag{3}$$

and the solution is given by:

$$Y = \frac{1}{x} \cdot \left[A \sin (kx) + B \cos (kx) \right] \quad . \tag{4}$$

The constants A and B are selected to meet the conditions at the stress-free boundaries at $x = x_1$ and $x = x_2$. These results lead to the following equation for the resonant lengths ($\ell = x_2 - x_1$) of the horn:

$$\text{Tan } (k\ell) = \frac{k\ell(N-1)^2}{(k\ell)^2N+(N-1)^2} \tag{5}$$

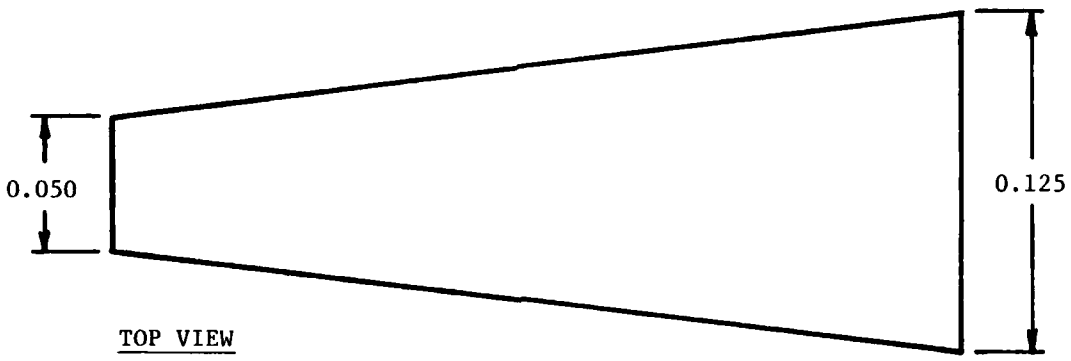

Dimensions In Inches

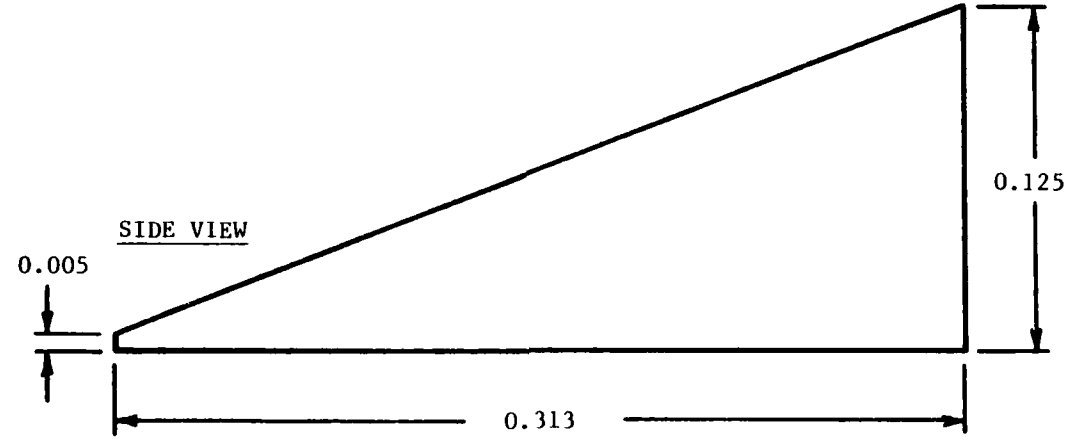

FIGURE 1. HALF WAVELENGTH, WEDGE-SHAPED HORN DESIGNED TO RESONATE AT 400 kHz

where

$$N = \sqrt{S_2/S_1} \tag{6}$$

and the S_i's are the areas at the x_i's.

However, the areas described do not lead to a square-law relationship between area and position. The case of the wedge which has this area relationship is when the ratios of the width to the thickness at any position are equal. Thus, for mathematical convenience the plane at x_i is assumed to be square with an area of 0.05 inch x 0.005 inch and therefore a length of 0.0158 inch. N in equation (6) is then equal to 7.91. The receiver was designed to match the flexural transmitter horn (described later) at 400 kHz.

The wave number is given by

$$k = \frac{\omega}{c_s} = \frac{2\pi f}{c_s} \tag{7}$$

where c_s is the speed of sound in steel. It equals $12.7(\text{in})^{-1}$. Substituting these values into equation (5) yields a half-wave length of 0.313 inch. This completes the wedge horn design.

To complete the receiver design, the following were added. Another half-wave length (0.25 inch) of the square stock was added to make the steel segment one wave length long at 400 kHz. The active element was a PZT-4 disk 0.1 inch in diameter and 0.08 inch long. A mixture of epoxy and copper was added behind the PZT-4 to act as damping material. The final design is shown in Figure 2a along with an impedance diagram in Figure 2b.

Transmitter (Unimorph Design)

In an effort to reduce the amount of space required by the probes, a new design of the transmitter was tried. This design was based on the flexural modes of a fixed free beam as shown in Figure 3. The fixed end would be the end that is mounted to the probe manipulator. The free end would be the end to contact the solder joint. Thus this model assumes that the contact of the

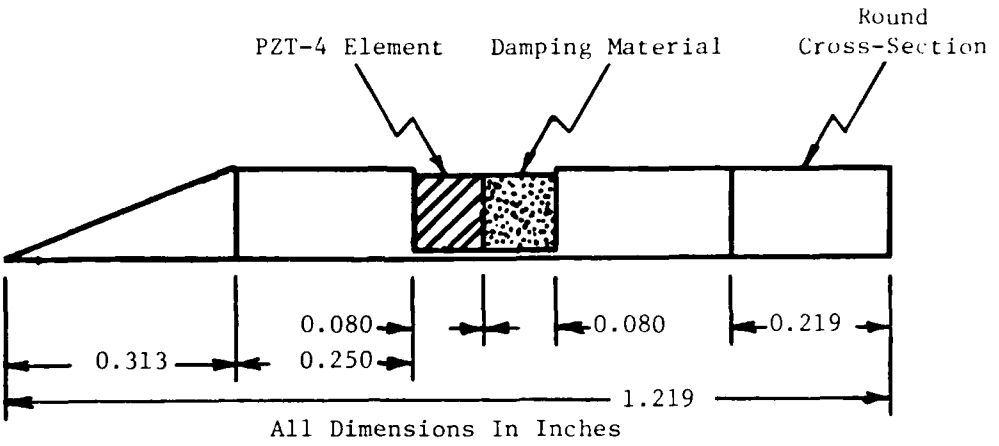

FIGURE 2a. WEDGE-SHAPED RECEIVER DESIGN

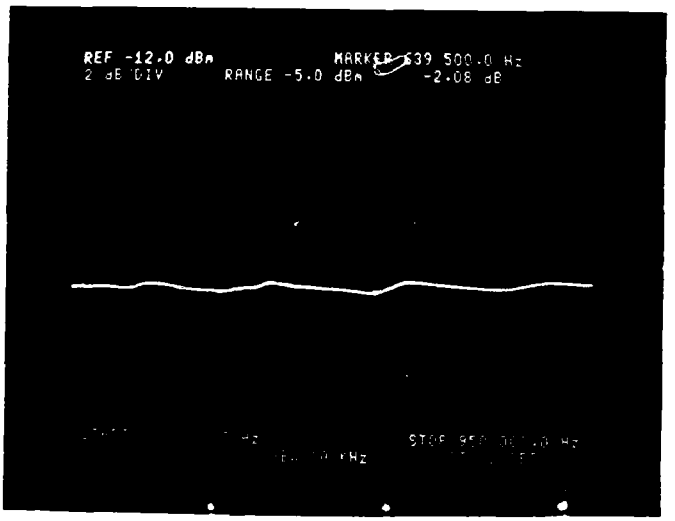

FIGURE 2b. IMPEDANCE DIAGRAM OF
WEDGE-SHAPED RECEIVER
($|Z|$ vs f)

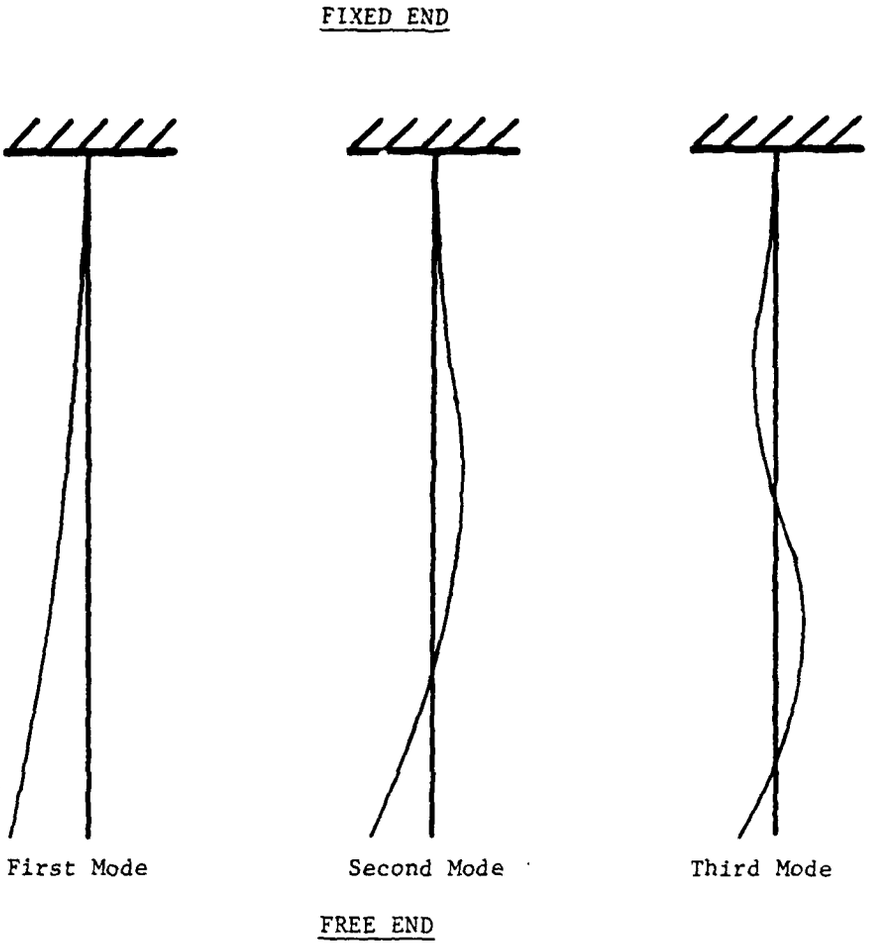

FIGURE 3. FLEXURAL MODES OF A BEAM WITH FIXED-FREE BOUNDARY CONDITIONS

joint and the probe does not impede the motion of the probe. In actuality, the end is coupled to the joint in order to transmit ultrasonic energy for inspection. However, as a first approach this would be sufficient to design the probe.

The following differential equation describes the amplitude of flexural vibrations of a beam:

$$\frac{d^4Y}{dx^4} = \frac{m'\omega^2}{EI} Y \tag{8}$$

where

Y is the amplitude of vibration,
x is the distance along the beam,
m' is the mass per unit length,
ω is the frequency of vibration, and
EI is the flexural rigidity.

The general solution of the differential equation is:

$$Y = A_1 \sin(kx) + A_2 \cos(kx) + A_3 \sinh(kx) + A_4 \cosh(kx) \tag{9}$$

where

$$k = \sqrt[4]{\frac{m'\omega^2}{EI}} \quad . \tag{10}$$

The coefficients, A_i, are determined by the boundary conditions. For the fixed end which is at x = 0, the displacement and slope of displacement must equal zero:

$$Y(0) = 0 \qquad \text{displacement} \tag{11}$$

$$dY/dx(0) = 0 \qquad \text{slope} \quad . \tag{12}$$

At the free end, $x = \ell$, the moment and shear must be zero:

$$EI\ d^2Y/_{dx^2}\ (\ell) = 0 \qquad \text{moment} \tag{13}$$

$$EI\ d^3Y/_{dx^3}\ (\ell) = 0 \qquad \text{shear force} \quad . \tag{14}$$

The boundary conditions can be summarized by the following matrix equation.

$$\begin{bmatrix} 0 & 1 & 0 & 1 \\ 1 & 0 & 1 & 0 \\ -\sin(k\ell) & -\cos(k\ell) & \sinh(k\ell) & \cosh(k\ell) \\ -\cos(k\ell) & \sin(k\ell) & \cosh(k\ell) & \sinh(k\ell) \end{bmatrix} \begin{bmatrix} A_1 \\ A_2 \\ A_3 \\ A_4 \end{bmatrix} = 0 \tag{15}$$

or simply

$$[A]\ \underline{C} = \underline{0}\ . \tag{16}$$

To determine the resonant frequencies of the beam, one determines which values of ω make the determinant of [A] zero. The following values for the resonant radian frequencies ω_n ($= 2\pi f_n$) result:

$$\omega_n = k_n^2 \sqrt{EI/m}, \tag{17}$$

where $k_n\ell = 1.875, 4.694, 7.855, 10.99$ for the first four modes of the beam. The above equation may be rearranged to solve for the length:

$$\ell = 0.2143\ (k_n\ell)\sqrt{\frac{ct}{f_n}} \tag{18}$$

where

t is the thickness of a rectangular beam,

c is the speed of sound, and

f_n is the resonant cyclic frequency.

At this point one must consider the practical aspects of the probe. The primary difference between the model and the probe is that the model to this point describes a uniform rectangular beam of a single material, whereas the probe is constructed of stainless steel and PZT-4. This type of construction to obtain flexural resonant modes in plates is known as unimorph. The difference between the model and the probe can be accounted for by proper selection of the thickness and length of the probe. The basic concept is to design the probe so

that the neutral plane of the beam coincides with the interface between the two materials. The following design procedure leads to that result.

(1) Select a commercially-available PZT element which is thin enough to obtain the desired frequency.

(2) Assume that the beam is made of two thicknesses of the PZT elements so that the neutral plane is at the mid-plane.

(3) Select the design frequency.

(4) Calculate the length of the beam to achieve that frequency [equation (18)]. Note, that different lengths will be obtained for the various modes. Once the length of beam is selected the width of the steel segment can be selected.

(5) Manipulate equation (18) to solve for t.

(6) Take the calculated width, t, of the beam and divide by two to obtain the thickness of the steel.

This procedure was used to obtain the dimensions shown in Figure 4a to operate in the second flexural mode.

As stated earlier, this design was developed to lower the amount of free area above the joint required to place the probe. As can be seen by the dimensions in Figure 4a, only a rectangular area of 0.132 inch by 0.050 inch is required for this probe.

A probe was constructed and impedance diagram of the probe was obtained with an HP3585A spectrum analyzer. It is shown in Figure 4b. The response was highly damped by the addition of damping material. The design resonance equalled 390 kHz but the resonance at 553 kHz was noted and roughly equalled the first longitudinal mode of the probe. That is, a standing stress wave existed between the free-face of the PZT and the free-face of the steel.

In order to improve the performance, the probe was modified so that both resonant modes, second flexural and first longitudinal, occurred at the same frequency. The easiest dimension to change on the existing probes was the length. By shortening the length of the beam the resonant frequency of the flexural mode could be increased to equal the frequency of longitudinal mode. By shortening the length to 0.192 inch the two modes both occurred at about 550 kHz.

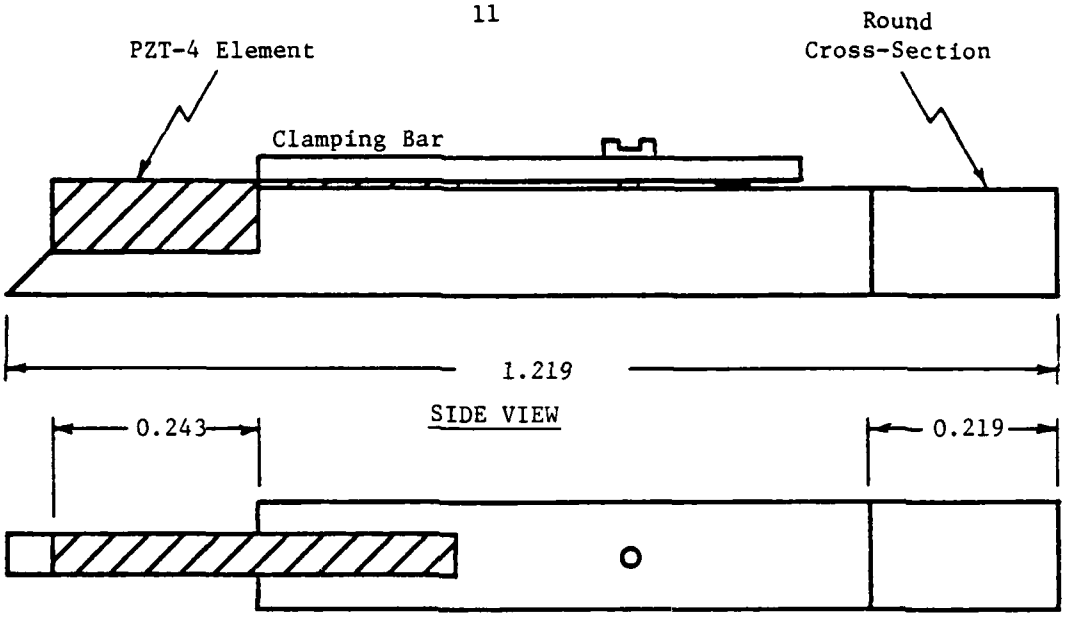

All Dimensions Are In Inches

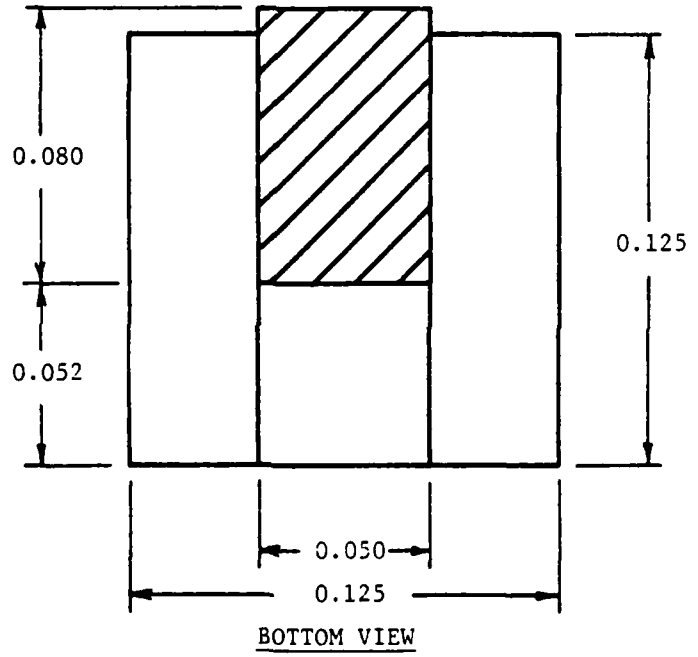

FIGURE 4a. DESIGN OF FLEXURAL-MODE TRANSMITTER

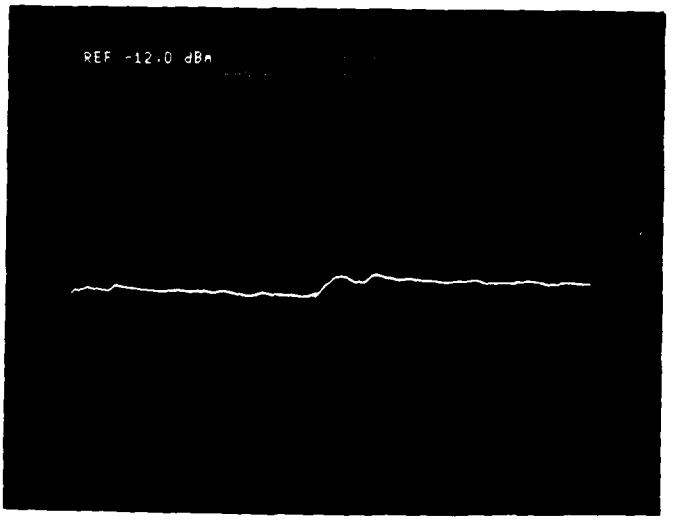

FIGURE 4b. IMPEDANCE DIAGRAM ($|Z|$ vs f) OF FLEXURAL-MODE TRANSMITTER

[Note response is highly damped due to the addition of damping material not shown in Figure 4a.]

The probe's performance was evaluated by inspecting a few joints on Board No. 5. While cracked joints did yield increased signal levels compared to good joints, the difference was not as dramatic as previous results with other probe sets. In part this was due to several other resonances which ocurred in the inspection frequency range. These components would contribute to the received signal but were not sensitive to joint condition. Thus they added more constant power to the signal so that the percentage difference in power between good and cracked joints was smaller and therefore detected less reliably.

Although the geometry of the probe was well-suited for a practical solder joint inspection station, the spectral performance was unsatisfactory. Therefore another transmitter was designed.

Transmitter (Longitudinal Design)

Since the best results in Phase 2.1 were obtained with a probe operating primarily in a longitudinal mode, another longitudinal transmitter was designed. This probe was designed to resonate at 500 kHz which is in the range of frequencies sensitive to joint condition. PZT-4 elements 0.1 inch in diameter and 0.1 inch thick are available. At this frequency a wavelength, λ, in PZT-4 is

$$\lambda = \frac{c_{PZT}}{f} = \frac{1.3 \times 10^5 \text{ in./sec}}{500 \times 10^3 \text{ cycles/sec}} \qquad (19)$$

$$\lambda = 0.26 \text{ in./cycle} \quad .$$

Thus the thickness of the PZT element is greater than 1/4 wavelength. This implies the nodal point of a 1/2 wavelength resonator would be within the element. The nodal point is a position of zero vibration and hence the point at which one mounts the transducer without significantly affecting the vibration. Since it is impractical to directly mount to the PZT element, the transducer was designed as a one wavelength resonator at 500 kHz. This ensured one nodal point within the steel segment of the probe by which it could be mounted.

The length of the steel segment was chosen so that the probe would be resonate at 500 kHz. The simplest model that can be used to determine the length is to state that to resonate at 500 kHz the time it takes a sound pulse to travel

from one end of the probe to the other must equal one period of vibration. The following expression results:

$$n \cdot \frac{1}{f} = \frac{\ell_s}{c_s} + \frac{\ell_{PZT}}{c_{PZT}} \tag{20}$$

where

ℓ_s is the length of the steel segment,

ℓ_{PZT} is the length of the PZT segment,

c_s is the speed of sound in steel,

c_{PZT} is the speed of sound in PZT-4,

f is the desired frequency, and

n is the number of cycles.

The length of the steel segment is calculated to be 0.243 inch. The nodal point in the steel occurs 0.099 inch away from the free steel face.

To contact the joint a small foot was added with a beveled point. The thickness of the foot at the transducer must be kept narrow enough so that it moves as a rigid body. A support stem was also designed and silver-soldered to the probe at the nodal point. The resulting design is shown in Figure 5a.

An impedance diagram of the probe is shown in Figure 5b. From this diagram, three areas of frequency contain significant resonant peaks. To better understand the origins of these peaks and the effect of design parameters on their location in frequency, a more detailed analysis was performed.

The model assumes that an n-layered transducer is constructed. The model only accounts for the longitudinal vibration in each layer. The general differential equation of motion in each layer is assumed to be:

$$\frac{d^2Y_i}{dx^2} + k_i Y_i = 0 \tag{21}$$

where

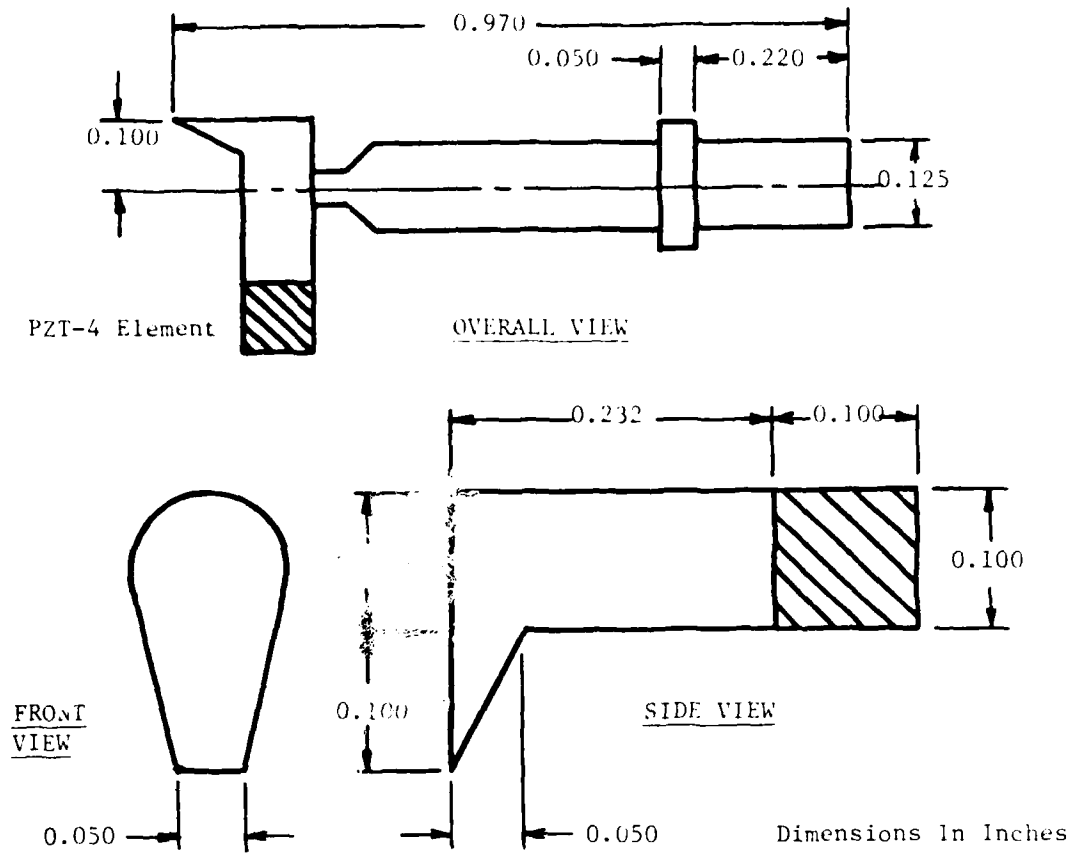

FIGURE 5a. LONGITUDINAL TRANSMITTER DESIGN

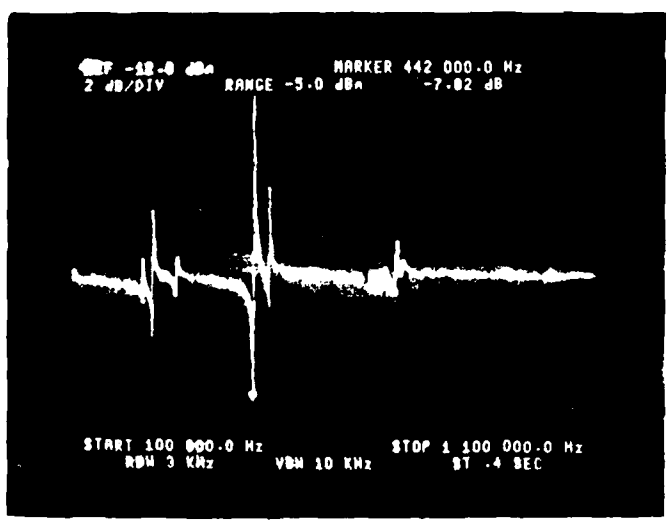

FIGURE 5b. IMPEDANCE DIAGRAM OF LONGITUDINAL TRANSMITTER
($|Z|$ vs f)

Y_i is the amplitude of vibration in the i^{th} layer,

x is the position, and

k_i is the wave number for the i^{th} layer.

The general solution is:

$$Y_i = A_i \sin(k_i x) + B_i \cos(k_i x) \tag{22}$$

where the A_i's and B_i's are constants determined by the boundary conditions. At the interface between two layers the following boundary conditions exist:

$$Y_i(d_i) = Y_{i+1}(d_i) \tag{23}$$

$$E_i A_i \frac{dY_i}{dx}(d_i) = E_{i+1} A_{i+1} \frac{dY_{i+1}}{dx}(d_i) \tag{24}$$

where

E_i is Young's Modulus of the material in the i^{th} layer,

d_i is the position of the interface between the i^{th} and $(i+1)^{th}$ layer.

The first condition states that the displacements must be equal and the second states that the forces must balance. Two additional boundary conditions exist at the free ends:

$$\frac{dY_1}{dx}(d_i) = 0 \tag{25}$$

$$\frac{dY_n}{dx}(d_{n+1}) = 0 \quad . \tag{26}$$

These state that no forces are exerted at the free ends. The above equations can be simply expressed by the matrix equation, [A] $\underline{C}$ = 0, shown in Figure 6.

The resonant frequencies are those values that make the determinant of [A] equal to zero. The resonant frequencies were determined by this method for two cases. The first case was a two layer model of PZT-4 and stainless steel. The second case was a three layer model which included a small layer of

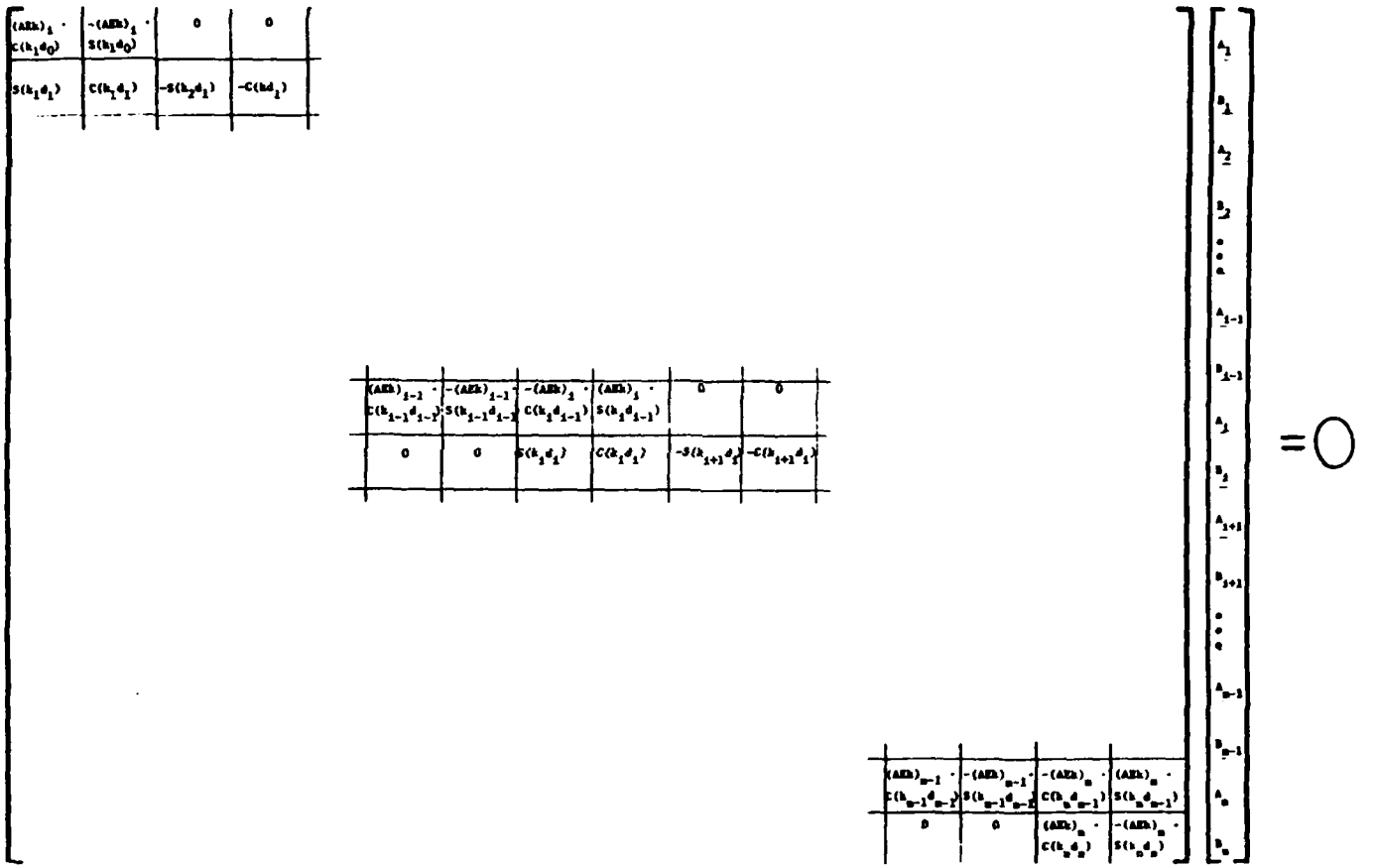

NOTE: $(AEk)_i = A_i E_i k_i$ $\quad S(x) = \sin(x)$ $\quad C(x) = \cos(x)$

All nonzero terms are shown in the six rows that appear.

FIGURE 6. MATRIX EQUATION [A] $\underline{C}$ = 0 WHICH DESCRIBES n LONGITUDINAL VIBRATIONS IN n LAYER DEVICE

solder between the PZT and steel which was used to fabricate the probe. The lengths and constants used for the model are listed in Table 1.

Two BASIC programs were developed for an HP-85 microcomputer. Both programs did searches for the frequencies within the range of 100 kHz to 1.1 MHz which lead to a value of zero for the determinant of [A]. The difference was that one contained a general determinant solver and the other had the determinant expressed as a single equation for the two layer case. The values observed with the impedance diagram and the two models are listed for comparison in Table 2. The frequencies taken from the impedance diagram are the strongest resonances within each of the three groups. Thus, the model seems to reasonably predict the frequency of the modes and may be used to analyze existing probes or in the design of new probes. As it is, this probe has three well-defined modes in the frequency range of inspection.

In addition to the three longitudinal modes predicted by the model, other modes are also observed. Since these are located in same regions as the thickness modes, they are presumably closely coupled modes. To eliminate some of these modes a mixture of epoxy and copper was made and added at the end of the PZT element. This is a damping material that lessens the amplitude but also broadens the response at the resonance. In addition heat shrink tubing was also added both to protect the probe and increase the damping. The damped impedance curve is shown in Figure 7. This probe was used along with the receiver probe previously discussed in performance definition experiments.

ANALYSIS/DECISION PROCEDURES

During ultrasonic inspection, a good/cracked decision is made based on information contained in the frequency response spectrum of the joint under test. As the frequency at which the joint is excited by the transmitter portion of the ultrasonic probe set is swept over a range (from low to high frequency), the amplitude of the joint response as detected by the receiver portion of the probe set is recorded. In the equipment presently used, approximately one thousand separate points, stored as 8-bit binary words, are used to describe the spectrum.

TABLE 1. CONSTANTS AND GEOMETRY USED IN THE MODEL FOR LAYERED LONGITUDINAL TRANSDUCERS

Material	Lengths		Speed of Sound (inch/second)	Young's Modulus (N/M^2)
	2 Layer (inches)	3 Layer (inches)		
Steel	0.232	0.234	1.98×10^5	2.07×10^{11}
Solder	--	0.003	0.73×10^5	3.18×10^{10}
PZT-4	0.100	0.100	1.29×10^5	8.15×10^{10}

TABLE 2. A COMPARISON OF THE OBSERVED AND THEORETICAL RESONANCE FREQUENCIES, kHz

Observed	Two-Layer Model	Three-Layer Model
257	268	258
442	494	483
720	788	771
---	1,013	974

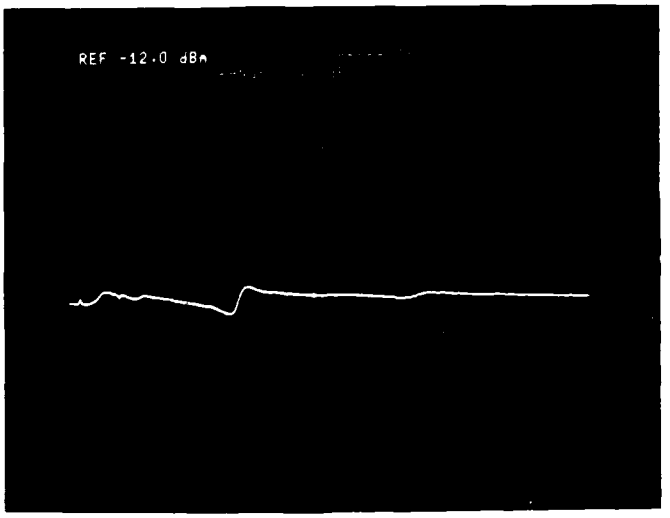

FIGURE 7. IMPEDANCE DIAGRAM OF LONGITUDINAL TRANSMITTER WITH DAMPING MATERIAL ADDED

[See Figure 5b for comparison to undamped case.]

The processing algorithm used to make a good/cracked decision has undergone several changes and developments during the course of the program. Four different approaches were used, with varying degrees of success depending on the particular transducer probe set used. The first technique developed made use of a resonance feature of an early transducer. Two sharp resonance peaks were seen in the lower half of the transducer characteristic spectrum whose location (frequency) was independent of joint quality. One of these peaks was used as a reference against which to judge the total area under the spectral curve.* A cracked joint exhibits a greater area than a good joint, all other things being equal. All points of the spectrum were summed to obtain the total area of the spectrum, and that number was then divided by the area of one of the transducer characteristic peaks to obtain a "quality factor" with which to make the good/cracked decision. The division by the reference area tended to null out any variations in coupling or joint compliance.

The next transducer design (the unimorph design discussed earlier) did not exhibit clearly defined resonances, making the technique just described unusable. Discussions with individuals making visual judgments using the new transducer indicated that spectrum peaks above some level were a good indicator of heel cracks in the joint under examination. Two algorithms were developed based on that information. The first merely detected the presence or absence of spectral peak amplitudes above a preselected level to make the good/cracked decision. Sensitivity to noise and lack of discrimination made this simple technique unsatisfactory. To improve performance, the algorithm was modified to make a decision based on the number of spectral peaks above a preselected level instead of simply on the basis of their presence or absence. The joints were called good until a preselected number of peaks above the level was exceeded. This algorithm provided significantly better performance.

The next transducer, similar to the one used in the present system, (the longitudinal design discussed earlier) provides a smoother spectrum than the previous versions. A decision may be made based on the total area of the spectrum alone. This is obtained by simply summing all of the spectrum point amplitudes. A value is set such that spectrum areas less than that value will indicate a

---

*This area is related to the power in the spectrum.

good joint and those greater will indicate a cracked joint. Good performance was obtained with this algorithm and transducer design, as discussed elsewhere in this report.

All of these processing techniques were implemented using a Motorola EXORciser I minicomputer, based on the 6800 microprocessor. The spectrum data is taken by a Hewlett-Packard model 3585A spectrum analyzer. Communication between the computer and the spectrum analyzer is accomplished by means of the IEEE-488 standard instrumentation data bus. After placement of the printed wiring board containing the joints to be inspected, the operator types the character "G" at the system console to start the automated inspection sequence. The ultrasonic probe is placed on the joint, the ultrasonic signal is applied to the transducer, the response spectrum data is taken and transferred to the computer, and a good/cracked decision is made, all automatically. The system is designed to be "operator friendly", allowing individuals with limited experience with computers to operate it. The operator is prompted by the computer at each step of the set up and operation sequences.

PILOT MODEL

A probe manipulator for the pilot model of the ultrasonic subsystem was designed and constructed during this contract period. Among the requirements set forth for this manipulator were a stroke of at least 1/2 inch, provision for the ultrasonic probes to be in contact with the solder joint for 50 milliseconds, a probe cycle time of 3 cycles per second, and a contact force between the probes and the solder joint between 10 and 16 grams during the inspection period.

Each probe is independently spring loaded to allow relative movement while in contact with the joint. Nominal probe contact force is 16 grams each and is adjustable to a minimum force of approximately 7 grams. In this design configuration the minimum contact force applied by each probe is a function of the weight of the probe carrier assembly. To allow for variations in solder joint and PC board height, the nominal contact force will be relatively constant through a vertical range of 1/16 inch. A drawing showing the manipulator configuration appears in Figure 8.

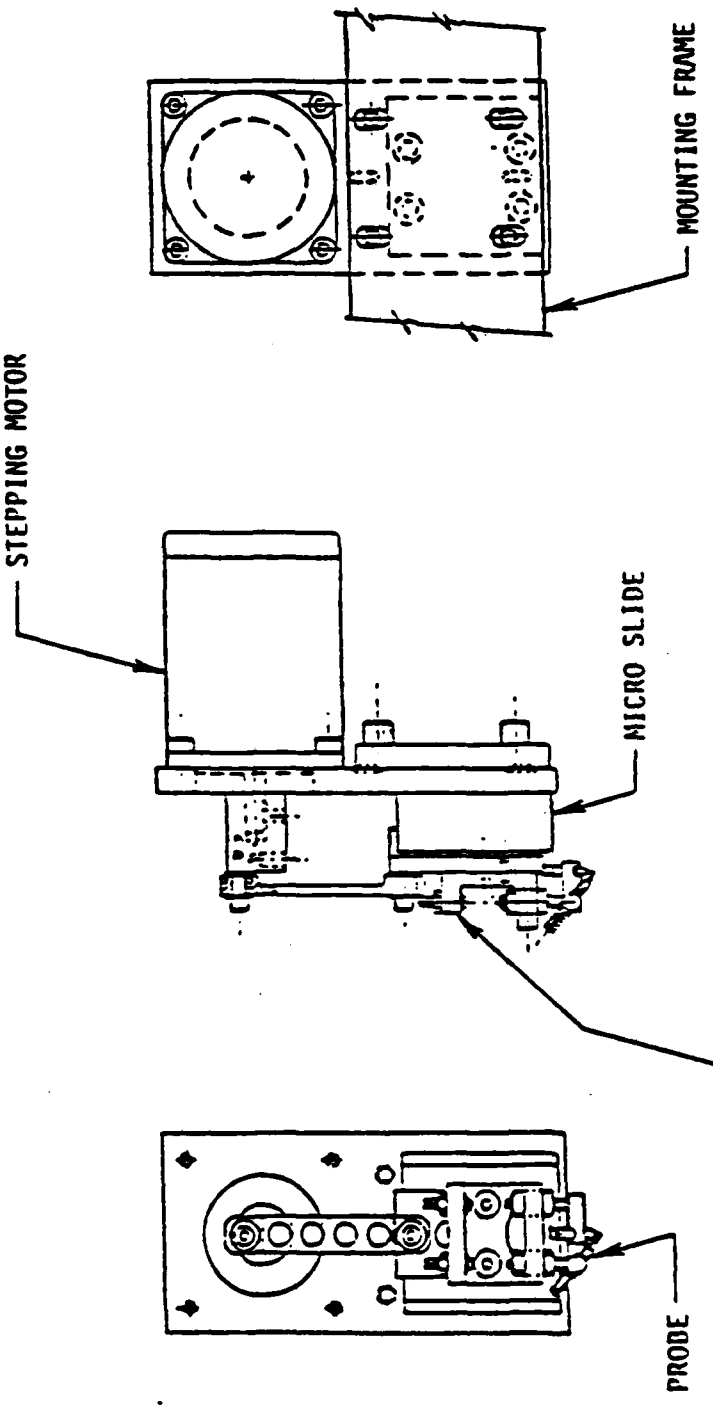

FIGURE 8. ULTRASONIC PROBE MANIPULATOR

For current experimental purposes the manipulator was mounted on a suitable frame support and base plate arrangement. This configuration consists of a base plate, upright supports, and a cross member for mounting the manipulator. A rotary indexing table is attached to the base plate to provide a surface for mounting sample PC boards. Figure 9 shows a drawing of this arrangement.

The probes are to be driven up and down by a stepper motor controlled from the same computer making decisions on joint quality. Because of difficulties with the motor control board in the computer, automation of the vertical motion of the probe manipulator was not completed in this contract period.

Figure 10 shows an operator at the computer terminal, the spectrum analyzer, and the probe manipulator mounted on its support system. Figure 11 shows a close up of the most recently designed and used probe set mounted in the manipulator and in contact with a solder joint.

PERFORMANCE DEFINITION AND IMPROVEMENT

Heel Cracks in Ribbon Lead Lap Joints

Sample Boards Nos. 4 and 5 were prepared during Phase 2.1 for use in evaluating video techniques in a demonstration held at Circon Corp. Each board contained 140 lap solder joints on flat pack ribbon leads. The boards as well as the leads were pretinned with solder. The solder joints were made using a hand iron to reflow the solder. In initial formation all of the joints were intended to be good. Subsequent to their formation, it was intended to create heel cracks in 56 randomly located joints on each of the two boards.

In order to generate some hard data on performance of the ultrasonic inspection technique using a large enough sample to be significant early in Phase 2.2 these two boards were subjected to inspection using the Phase 1 ultrasonic probe set. The staff performing the inspection had no knowledge of which joints were intended to be defective and which were not. In carrying out the experiment, the probe set was mounted on a phonograph tone arm and was placed on the joint under inspection by hand. The ultrasonic spectrum was displayed on a CRT and visually evaluated to make a good/bad decision on the joint's

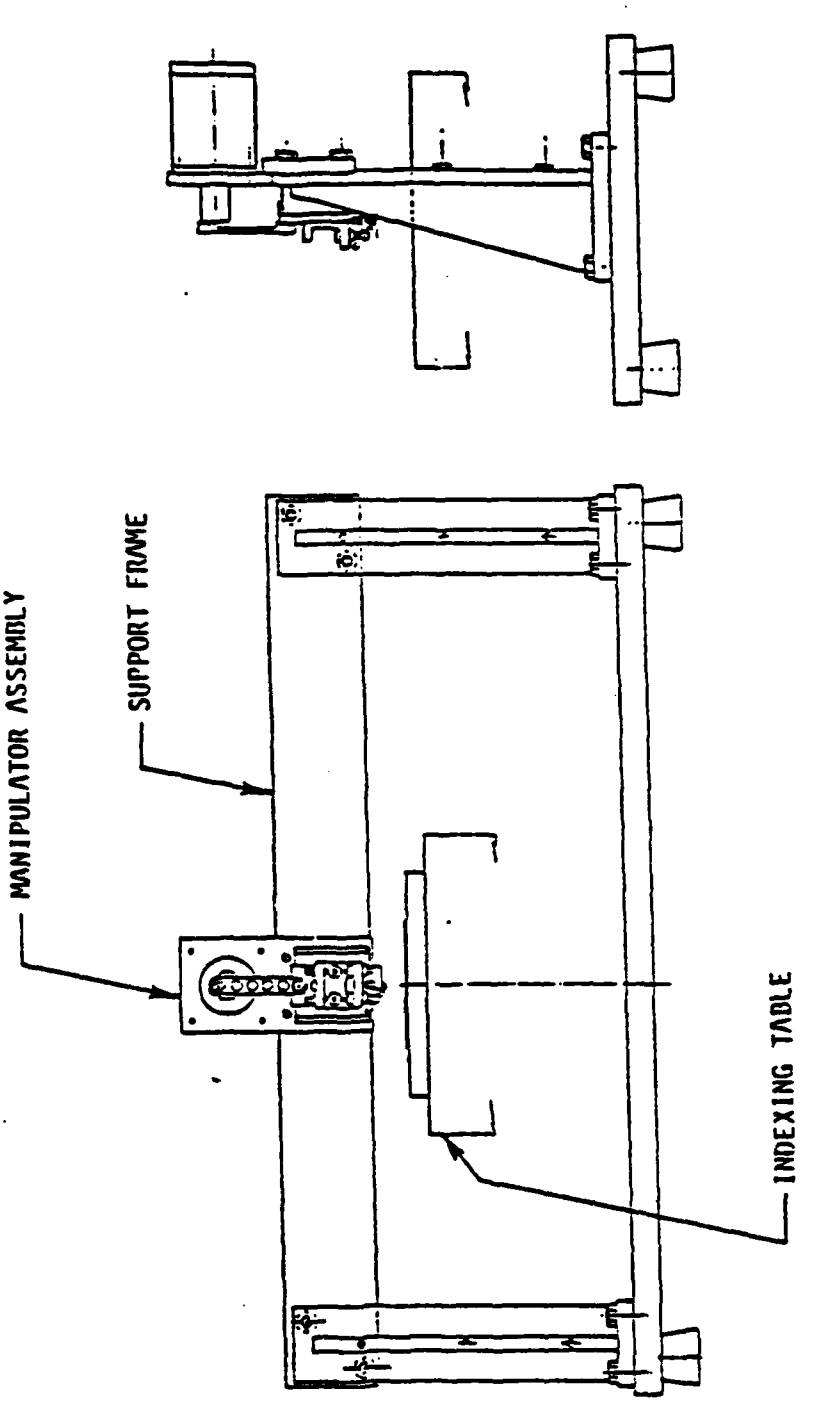

FIGURE 9. PROBE MANIPULATOR AND SUPPORT ARRANGEMENT

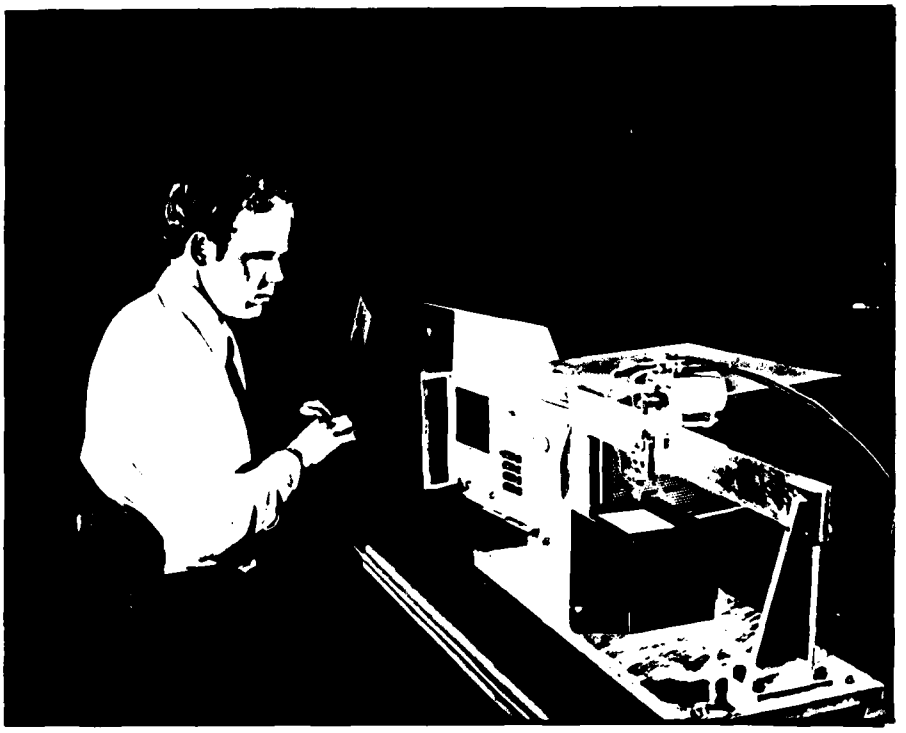

FIGURE 10. PROBE MANIPULATOR ON ITS SUPPORT SYSTEM WITH THE SPECTRUM ANALYZER AND COMPUTER TERMINAL

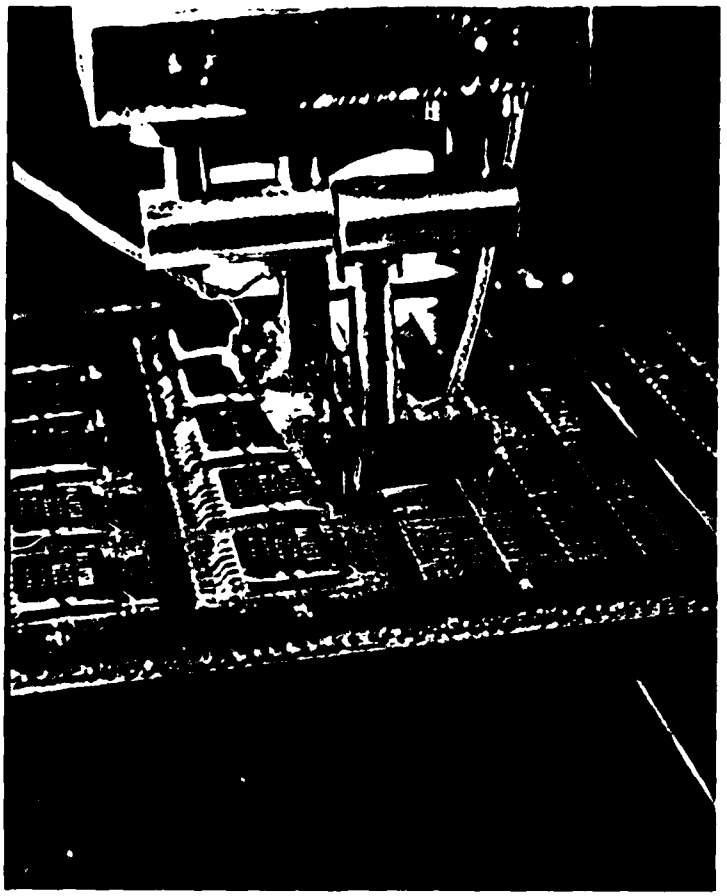

FIGURE 11. CLOSEUP OF THE LATEST PROBE SET MOUNTED ON THE MANIPULATOR

quality. The quality of most of the joints was recorded as G for good or B for bad, however a few qualified judgments were also made. A G^- or B^- indicated good or bad with some lack of confidence. A G^A or B^A indicated a good or bad joint but with the observation of some anomalous character in its spectrum. Microscopic inspection of the joints revealed that two which were supposed to have been cracked were not cracked. Thus, taking both boards into account there were 110 cracked joints and 170 nominally good joints subjected to the inspection. Table 3 shows the results of this experiment. Of 110 joints with cracked heels, 98 percent (all but 2) were correctly identified. Of 170 nominally good joints, 5 percent, or 8, were identified as defective.

The Engineering Specification for Phase 2.2 identifies as a preliminary goal for the ultrasonic inspection technique ". . . that not over 0.5 percent of good test joints shall be misidentified as cracked joints during automatic pilot model inspection of good test joints and defect type test joints." In other words, defining for purposes of this discussion a "false alarm" as a good lap solder joint incorrectly identified as a cracked joint, the false alarm rate in inspecting good joints should be no greater than 0.5 percent.

Demonstration of performance in relation to this goal requires a determination of the number of samples which must be inspected.

First consider the problem of how many good joints must be inspected, without the occurrence of any false alarms, in order to conclude, with 99.5 percent confidence, that the probability of a false alarm does not exceed 0.005.

Let q denote the proportion of good joints that will generate false alarms. Then $p = 1 - q$ denotes the proportion of good joints that will not generate false alarms. In a random sample of size n, the probability of exactly k false alarms is given by

$$\binom{n}{k} p^k q^{n-k} \quad , \tag{27}$$

where the binomial coefficient $\binom{n}{k}$ denotes the number of ways k false alarms could occur in a sample of size n. The probability of at least one false alarm is then given by

$$P = \sum_{k=1}^{n} \binom{n}{k} p^k q^{n-k} \quad . \tag{28}$$

TABLE 3. PERFORMANCE RESULTS FROM ULTRASONIC INSPECTION OF BOARDS NOS. 4 and 5[a]

Joint Quality From Microscopic Inspection	Number of Joints Inspected	Number Joints Declared[b]							Total Number Joints Judged[c]		
		B	B^-	B^A	B^{-A}	G	G^-	G^A	Defective	Good	Percent Correct
Heel Cracks	110	$51/_{43}$	$1/_2$	$3/_5$	$0/_3$	$1/_1$	---	---	108	2	98%
Good	170	$3/_0$	$3/_0$	---	$0/_2$	$69/_{76}$	$6/_0$	$3/_8$	8	162	95%

(a) For data presented in form $^{x}/_{y}$, x is from Board No. 4 and y is from Board No. 5.

(b) B = bad
G = good
B^- or G^- indicates some lack of confidence
B^A or G^A indicates some anomalous character in spectrum.

(c) All B, B^-, B^A, and B^{-A} counted as defective
All G, G^-, and G^A counted as good.

It is desired to choose the sample size n sufficiently large so that, if the false alarm proportion exceeds $P_o = 0.005$, then the probability of observing at least one false alarm is given by $P_o = 0.995$. That is, the following equation must be solved for n:

$$P = \sum_{k=1}^{n} \binom{n}{k} (0.005)^k (0.995)^{n-k} = 0.995 \quad . \tag{29}$$

This equation is easily solved by noting that the binomial distribution sums to unity for k = 0, 1, . . ., n so that

$$P + \binom{n}{o} (0.005)^o (0.995)^{n-o} = 1.0 \quad . \tag{30}$$

It follows that

$$P = 1 - (0.995)^n = 0.995 \tag{31}$$

and the required sample size is given by

$$n = \frac{\ell n\ 0.005}{\ell n\ 0.995} = 1058 \quad . \tag{32}$$

Thus, if a random sample of 1058 good joints are inspected and no false alarms are obtained, it may be concluded, with 99.5 percent confidence, that the proportion of false alarms is less than 0.5 percent in a large population of good joints.

To be more general the preceding equation can be written

$$n = \left. \frac{\ell n\ (1-c)}{\ell n\ P} \right|_{P = 0.995} \tag{33}$$

where c is the confidence level. From this a calculation can be made of the sample size required to demonstrate a proportion of false alarms less than 0.5 percent for different levels of confidence. Table 4 shows a few examples.

The experiment to demonstrate false alarm rate was planned for about the 80 percent confidence level.

TABLE 4. NUMBER OF SAMPLES REQUIRED TO DEMONSTRATE A FALSE ALARM RATE OF LESS THAN 0.5 PERCENT AT LISTED LEVELS OF CONFIDENCE

Confidence Level, c	Required Sample Size, n
0.995	1,058
0.99	919
0.95	598
0.90	460
0.80	322

The object of this experiment was to demonstrate the ability of the ultrasonic inspection system to perform the inspection of good joints with a satisfactorily low false alarm rate. To lend credibility to the demonstration, it was judged desirable to include among the joints inspected a sampling of joints with heel cracks in order to show that whatever performance is achieved in the inspection of good joints, it is achieved using inspection criteria which simultaneously permit the identification of cracked joints. A total of 420 lap solder joints on flat packs were used in this experiment. Of those 370 were nominally good and 50 were cracked.

In carrying out the experiment, the new longitudinal transmitter discussed earlier in this report was used. The probe set was mounted in the probe manipulator. The sample boards were mounted on a rotary indexing table. Once properly aligned, the table was manually advanced for inspection of each joint in a given row. At the time the experiment was run, it was not yet possible to actuate the stepper motor in the probe manipulator to vertically move the probes. This function was performed by rotating the stepper motor by hand. Thus the probe positioning should have been similar to that achieved by automatic placement except for the speed of placement.

For each joint inspected a computer generated good/bad decision was displayed on a CRT. Simultaneously but without a knowledge of the computer decision, an operator recorded a good/bad decision based on a visual examination of the displayed spectrum. Figures 12 and 13 show typical spectra from the probe set used in this experiment. Note the similarity between the spectrum from a good joint and the spectrum from an empty but pretinned soldering pad. Out of the 420 joints inspected, there was only one instance of an outright disagreement between machine decision and visual decision. In that instance the machine decision was wrong. A joint exhibiting a short crack was declared good. There were a few cases for which the joint under inspection was believed to have a somewhat anomalous spectrum visually but nevertheless placed in the good category. Results of this experiment, based on machine generated decisions only, are shown in Table 5. It will be noted that there was only one false alarm in the inspection of 370 good joints, for an observed false alarm rate of only 0.27 percent, a performance better than the preliminary goal. While achieving this level of performance in the inspection of good joints, all but one, or

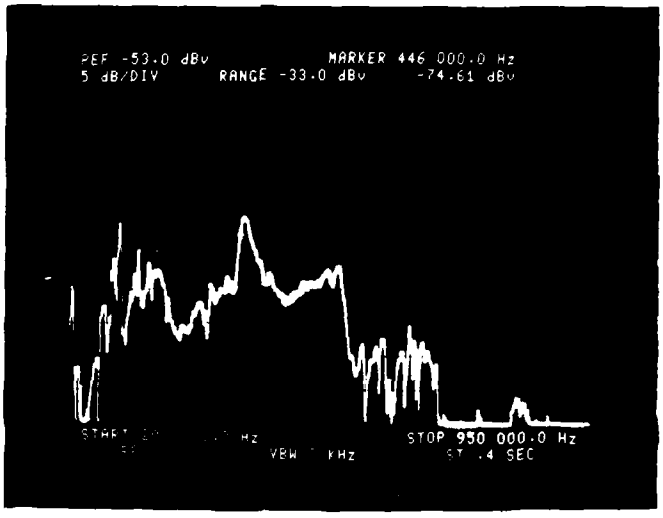

FIGURE 12a. Empty Solder-Coated Bonding Pad on Board 81-1

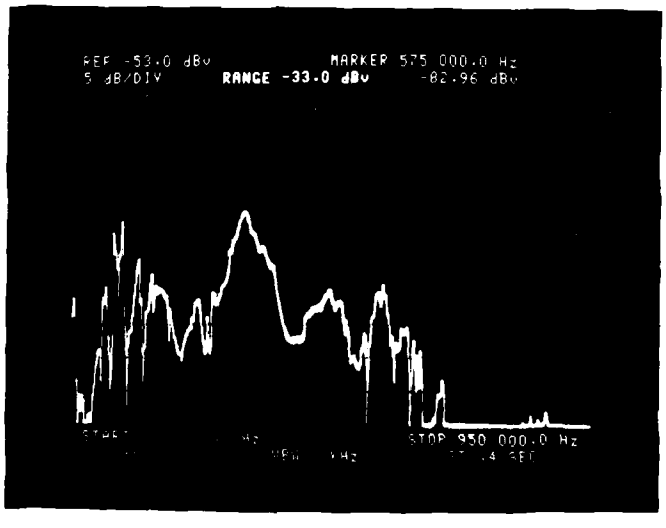

FIGURE 12b. A Good Joint (J1-1) on Board 81-1

FIGURE 12. TYPICAL SPECTRA FROM THE CURRENTLY USED ULTRASONIC PROBE SET

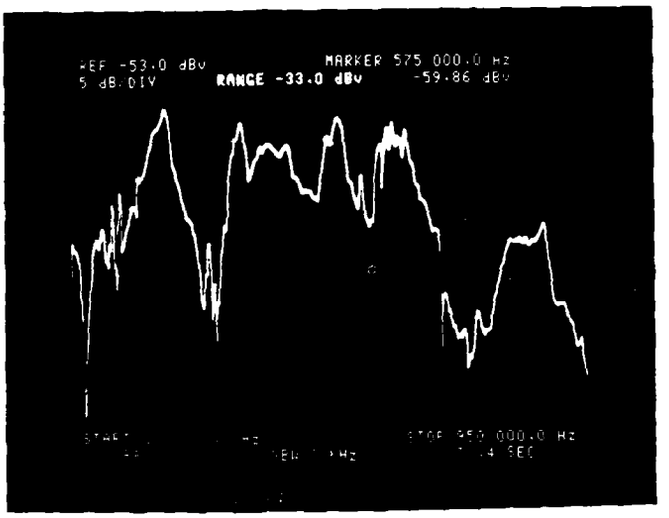

FIGURE 13a. Heel Crack in Joint E1-4 on Board 81-1

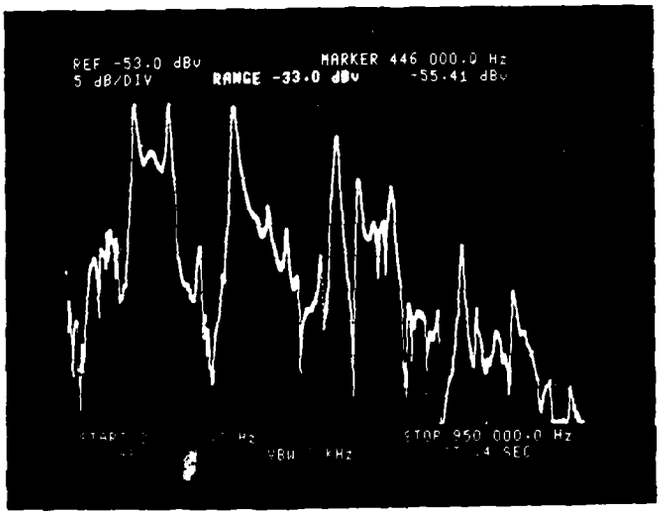

FIGURE 13b. Debonded Soldering Pad on Joint J4-2 on Board 81-1

FIGURE 13. SAMPLE SPECTRA GENERATED WITH THE CURRENTLY USED ULTRASONIC PROBE SET ON FAULTY JOINTS

TABLE 5. RESULTS OF EXPERIMENT TO DEMONSTRATE FALSE ALARM
(BASED ON COMPUTER GENERATED DECISIONS)

Joint Quality From Microscopic Inspection	Number of Joints Inspected	Number of Joints Declared Good	Number of Joints Declared Cracked	Observed False Alarm Rate (Percent)	Observed Miss Rate (Percent)
Good	370	369	1	0.27	NA*
Heel Cracks	50	1	49	NA*	2

*NA means not applicable.

98 percent, of the 50 joints with heel cracks inspected were properly identified as faulty.

The computer-generated data from this experiment are plotted in the histogram shown in Figure 14. The numbers on the horizontal axis are proportional to the power in the received signal or to the area under the joint's spectrum as determined by computer integration.* The height of the bars shows the number of joints in the indicated interval. For example there were 17 joints which had an area-related parameter between 39 and 40. There were no joints with an area-related parameter between 50 and 51.

The system threshold for differentiating between good joints and joints with heel cracks was set at 46. In other words all joints exhibiting a parameter below 46 were declared good by the system. All joints exhibiting a parameter of 46 or above were concluded by the system to have heel cracks.

The one false alarm generated (i.e., good joint declared cracked) was for joint A1-1 on Board 81-2. It had a paramter of 46.3, just above the threshold. It had a soldering pad partially lifted on one side which may have contributed to the large signal. The joints were all inspected to see if there were other partially lifted pads. Joint E4-1 on Board 81-1 was observed to have a partially lifted pad. Its parameter was 45.3, quite high for a good joint.

With the way joints are distributed on the parameter scale it is evident that a shift of threshold to a slightly higher level would reduce still further the liklihood of generating false alarms without creating a large increase in misses.

The mean parameter value for good joints occurs at about 34. There is a degree of symmetry observed in the distribution of joints about this mean. The distribution does not appear to be Gaussian. If the symmetry is in fact real its significance is as yet unidentified.

---

*"OF" indicates overflow of the computer register. In terms of the numbers used for this histogram overflow occurred above about 65.6. The system was programmed to classify as defective any joint whose spectrum resulted in an overflow condition.

Ⓐ Area-related parameter value of a cracked joint declared good (a miss).

Ⓑ Area-related parameter value of a good joint with corner of soldering pad debonded.

Ⓒ Area-related parameter value of a good joint declared cracked. (Classed as a false alarm.) One edge of the soldering pad was partially debonded.

Ⓓ Area-related paramter value of a cracked joint with a completely debonded soldering pad.

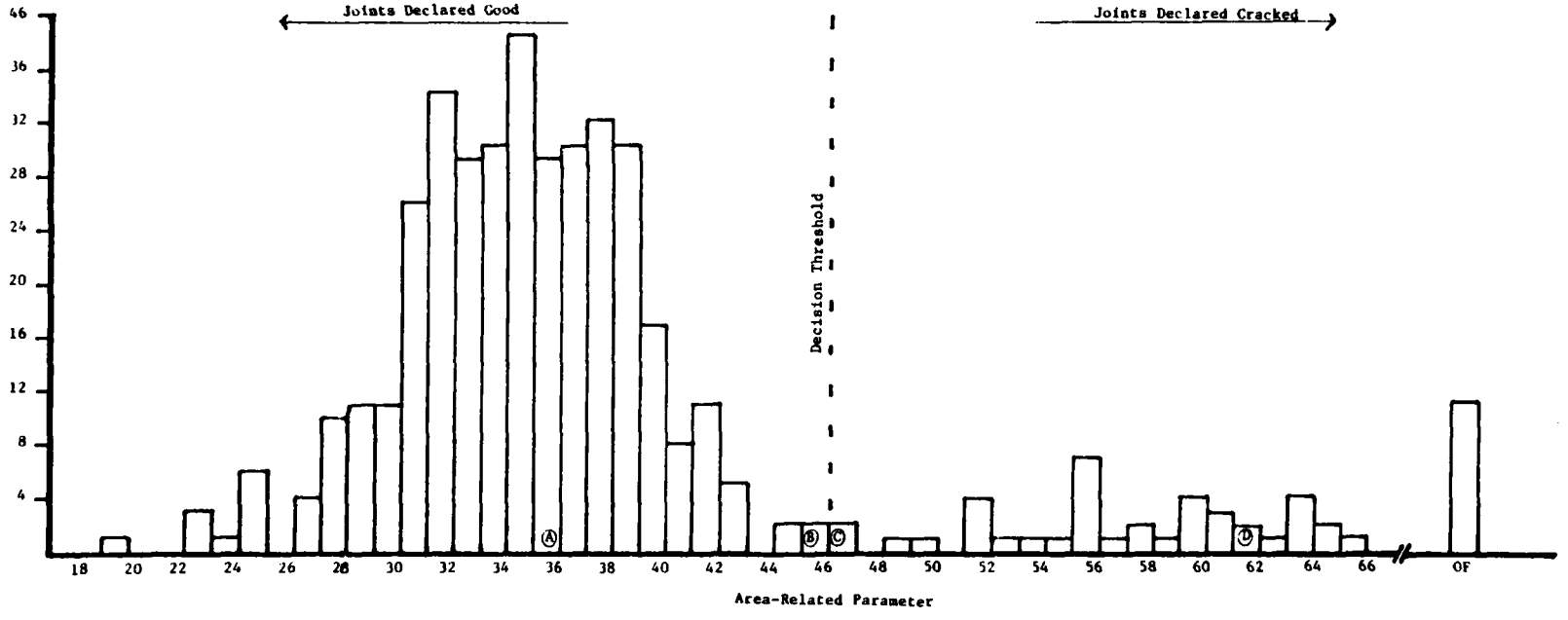

FIGURE 14. HISTOGRAM OF RESULTS OF INSPECTING GOOD AND HEEL CRACKED LAP SOLDER JOINTS ON FLAT PACK RIBBON LEADS [Based on Computer-Generated Decisions.]

Other Defect Types

Limited experimentation was carried out on a set of lap solder joints on ribbon leads containing examples of voids and cold joints as well as good joints and joints with heel cracks. There were 11 cracked joints, 18 good joints, 10 cold joints, and 17 joints with voids. The voids were made by drilling a 15 mil hole through the solder pad and its overlying presolder into the printed circuit board material. Subsequently a joint was formed in the usual way with the lead covering the hole. Some experimental joints made in this way were torn apart to confirm that the voids survived the soldering process.

The cold joints were made using the usual reflow technique but with inadequate heat to bring the joint parts to proper temperature and to properly flow the solder. With the decision threshold located at the same place as discussed earlier in this section, the system declared 4 of the 10 cold joints faulty.

Of the 17 joints containing voids only one was declared faulty on the basis of the established threshold. It was noted, however, that at least 10 of the 17 joints had an unusually high peak in their spectra falling between about 448 and 460 kHz. Of the remainder of the 56 joints in this experiment, only one or two displayed a similar peak. It is not possible with the information available to draw any positive conclusions about the significance of that peak in relation to the type of defective joint in which it frequently appeared. It would, however, be worth further investigation if that defect type is a subject of future study.

EXTENSION OF THE ULTRASONIC TECHNIQUE TO THE INSPECTION OF ALL LAP SOLDER JOINTS

Thus far in this program, attention has been directed exclusively to lap solder joints on ribbon leads, a lead type used on integrated circuit flat packs. The leads on resistors, capacitors, and other components are commonly round and of varying diameters. Sometimes the round leads are coined by the manufacturer to a common maximum thickness. The ultimate inspection system should be able to accommodate round and coined leads as well as ribbon leads.

As an initial step in developing this capability, a set of sample joints using 25 mil diameter round resistor leads was prepared to gain some insight into the performance of the system on this type of joint. A total of 32 joints were prepared of which 15 were cracked. Their general manner of preparation was similar to that which has been used for ribbon leads. These joints were inspected using the same probe set used in the experiments discussed in the immediately preceding section. Decisions were made automatically with the decision threshold at the same location. Figures 15 and 16 exhibit, respectively, two sample spectra of good joints and two sample spectra of joints with heel cracks in these round leads.

Figure 17 shows a histogram of the results of these inspections. It will be seen that all of the nominally good joints were properly declared good. Ten of the 15 joints with heel cracks were declared faulty.* While this performance does not approach that achieved on good and cracked joints in ribbon leads, it does provide a basis for optimism regarding the possibility of broadening the system's capability to adequately accommodate leads of varying shapes, sizes, mass, and materials.

RISK ASSESSMENT

While the ultrasonic inspection technique is nondestructive in nature, energy is being imparted to the components under test which if sufficient might damage the component. To assess the potential for IC damage the following studies were performed.

In one study, the receiver and transmitter, which were the original probe set, were placed on several locations on the IC package. In this way the relative displacements at various positions could be determined. Six positions were assigned numbers as indicated in Figure 18a. Positions 1 and 2 are the normal positions for the transmitter and receiver respectively. Position 6 is in the center of the floor of the IC package where the IC die would be mounted.

*One of the joints intended to be good was declared defective by the system. A careful microscopic examination of the joint revealed it to contain a fine heel crack which had not been artifically introduced.

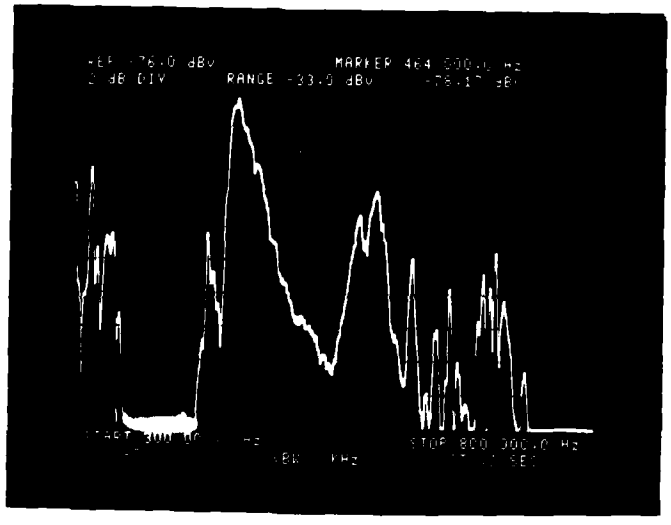

FIGURE 15a. Joint H4-2 on Board 81-A

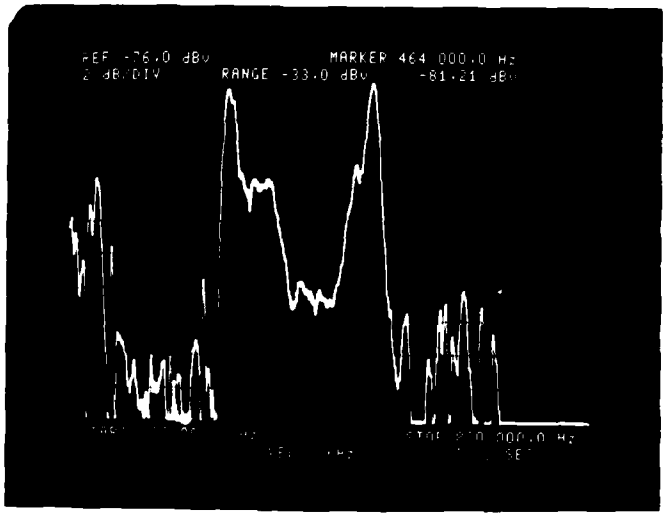

FIGURE 15b. Joint B1-2 on Board 81-A

FIGURE 15. TYPICAL SPECTRA OF GOOD LAP JOINTS ON 25 MIL DIAMETER ROUND RESISTOR LEADS

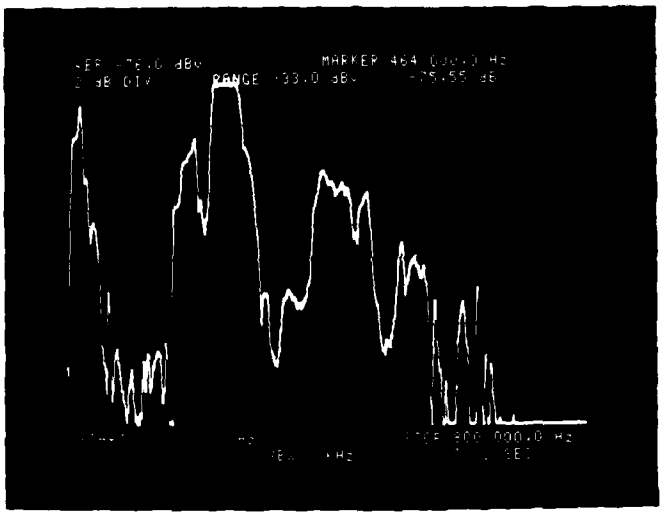

FIGURE 16a. Joint H1-2 on Board 81-A

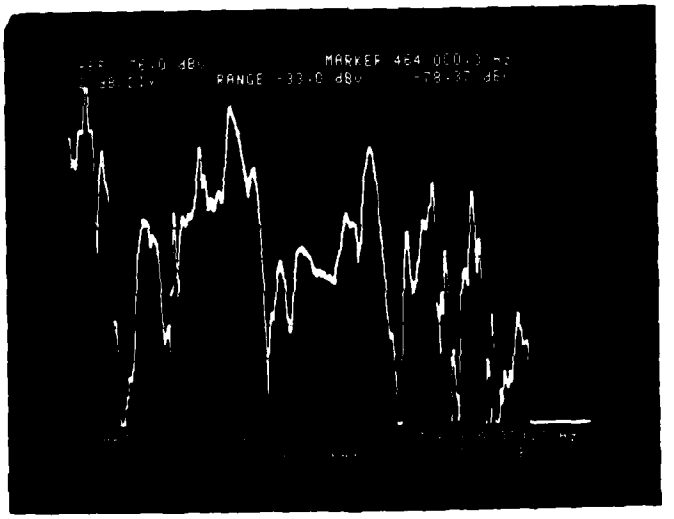

FIGURE 16b. Joint F2-2 on Board 81-A

FIGURE 16. TYPICAL SPECTRA OF HEEL CRACKED LAP JOINTS ON 25 MIL DIAMETER ROUND RESISTOR LEADS

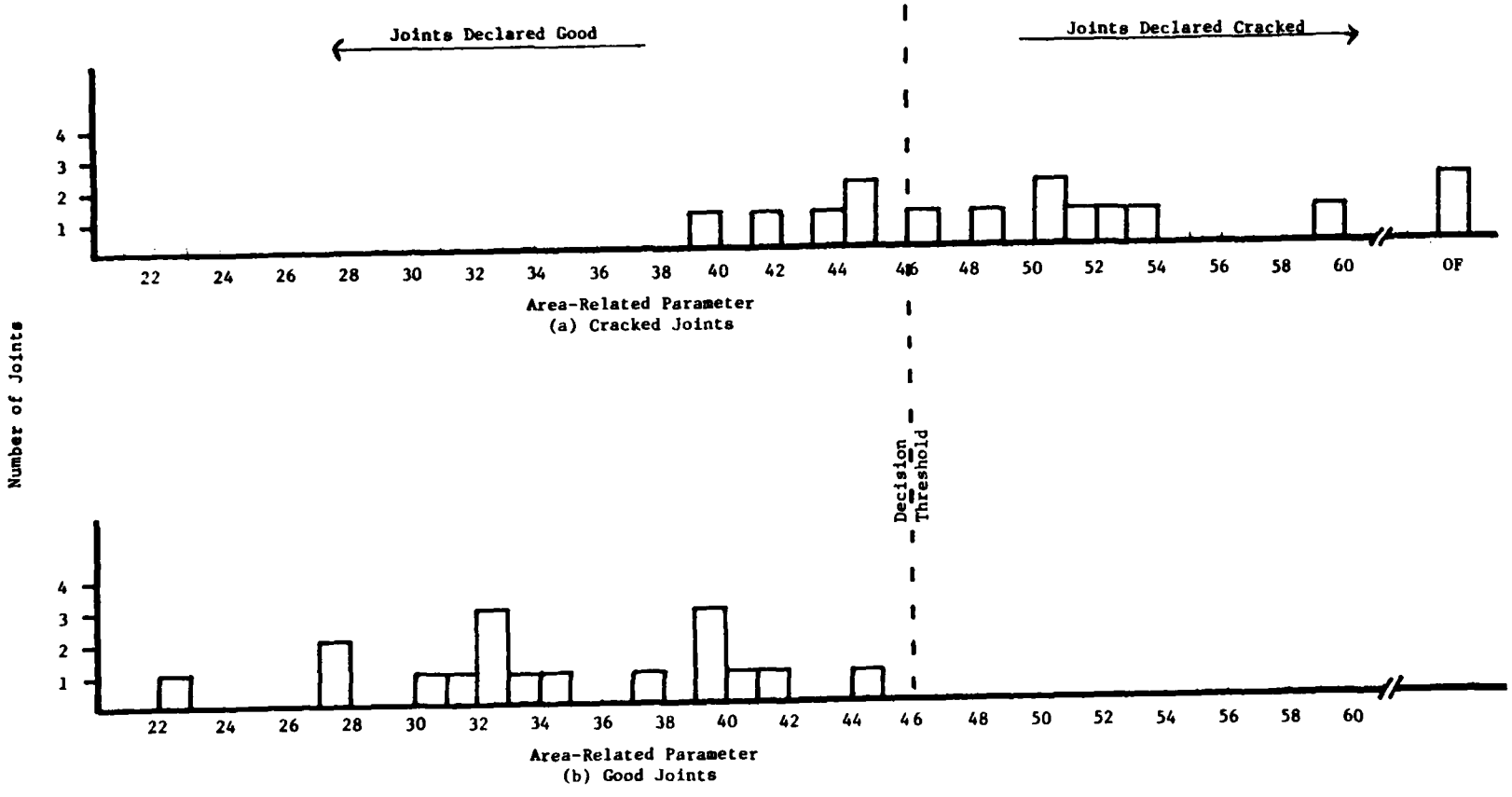

FIGURE 17. HISTOGRAM OF RESULTS OF INSPECTING GOOD AND HEEL CRACKED LAP SOLDER JOINTS ON 25 MIL ROUND RESISTOR LEADS

[Based on Computer-Generated Decisions.]

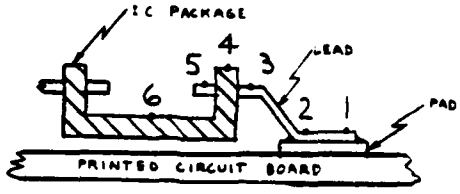

PROBE POSITIONS

Figure 18a. Probe Positions

GOOD JOINT

T ↓	R_1	R_2	R_3	R_4	R_5	R_6
T_1	Does Not Apply	-62* (Normal)	-75	-85	-87	-80
T_2	-67	Does Not Apply	Does Not Apply	-58	-58	-48

T = TRANSMITTER R = RECEIVER NUMBER = POSITION * = IN dB

CRACKED JOINT

T	R_1	R_2	R_3	R_4	R_5	R_6
T_1	Does Not Apply	-70	-78	-87	-86	-85
T_3	-71	Does Not Apply	Does Not Apply	-71	-55	-48

Figure 18b. Received Signals

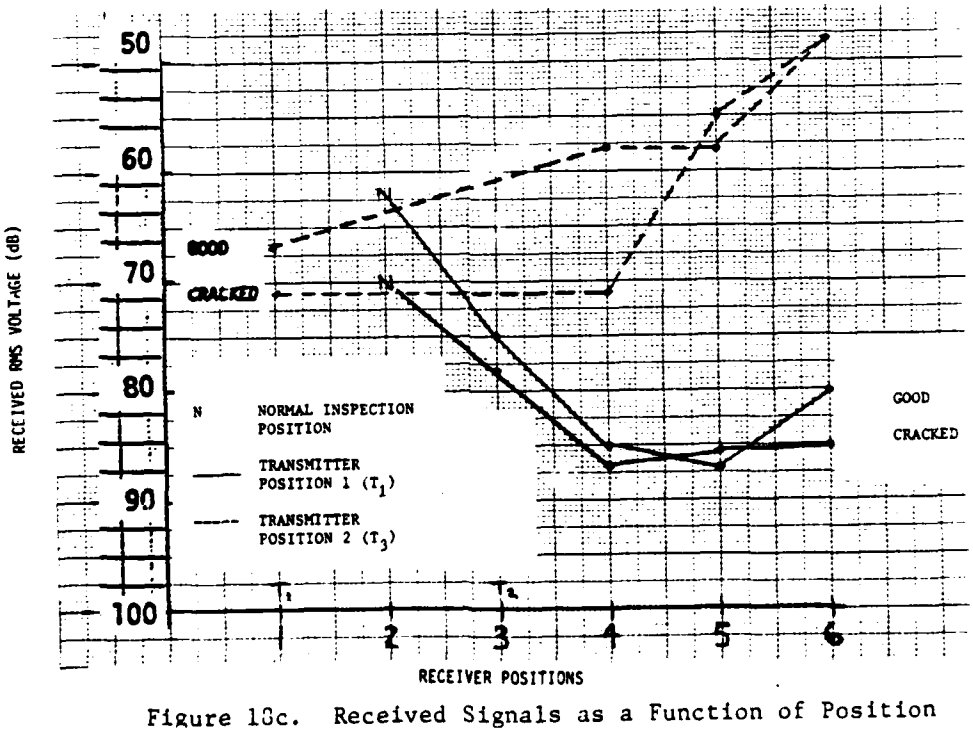

Figure 18c. Received Signals as a Function of Position

FIGURE 18. DATA ON ULTRASONIC ENERGY TRANSMISSION INTO AN IC PACKAGE.

The transmitter was placed in one of two locations; its normal inspection position (No. 1) and on the lead just outside the IC case (No. 3). The latter position represents a misplacement which might accidentally occur in actual practice. The drive signal to the transmitter was fixed for all tests. The receiver was placed on the remaining positions and the received spectra were obtained. These measurements were made for two joints, one good and one with a crack (C2-1 and C2-4 on printed circuit board No. 3 respectively.) The cracked joint was tested since generally more energy is contained within the lead. Thus the chance of damage may be greater.

An average rms voltage in the neighborhood of 265 kHz was determined for each transmitter-receiver configuration. This frequency corresponded to a transmitter resonance and the received signal at this frequency was very repeatable. These data, in dB, are listed in Figure 18b. Note, that the received signal for the cracked joint is generally lower than that for the good joint which is contrary to the basic differences in received spectra. However, this is not the case. This difference results because the voltages are determined for a narrow band about a specific frequency. The received spectra for these two joints over the entire inspection range of frequency are as typically observed for good and cracked joints.

The data from Figure 18b are plotted as a function of position number in Figure 18c. The results show that the signal is attenuated by 15 to 20 dB inside the IC package (positions No. 5 and No. 6 compared to position No. 2) with the transmitter in the normal position (No. 1). When the transmitter is placed on the lead near the case, the signal tends to increase inside the case. This may be due to the excitation of some modes of vibration of the floor of the IC package. It is doubtful that in a functional IC this condition would exist.

An experiment was designed to determine the signal power levels necessary to fail an IC. To do this quad nand gates (#MC2101F) were mounted on a PCB. The inputs were connected to a common input. Each lead would be driven by a resonant ultrasonic driver for a fixed amount of time. The drive power would be increased until the lead failed (cut) or the IC no longer functioned.

The outcome for a given trial would be the drive signal expressed as a ratio to the normal inspection levels at which the failure occurred. A number of trials would be performed to obtain a histogram of number of failures versus

power level. It was anticipated that it would be bimodal. That is it would contain two peaks, one due to IC failures and one due to lead failures.

To be a representative test, the frequency of the resonant ultrasonic driver should be within the normal inspection range. Therefore two probes were designed and constructed to handle the power and operate in the 100 kHz to 1 MHz range.

The first probe shown in Figure 19a was a 1/4 inch in diameter and roughly 1/2 inch long. The volume of the PZT elements was roughly 8 times greater than the normal transmitter probe. This implies that the probe could handle 8 times the power. While the impedance curve (Figure 19b) did indicate several large resonances in the range of 100 kHz to 1 MHz, none of these seemed to be the longitudinal mode for which the probe was designed. The probe was driven at the larger modes on an empty pad as a test. When viewed under a microscope no cutting action could be observed. Even at power levels sufficient to fail the probe (at the interface of the PZT elements and the steel segments) no cutting was distinguishable. Several modifications to the probe were made, however none improved the amount of cutting at the tip.

A second probe was designed and constructed that was narrower than the previous power probe (Figure 20a). This seemed to eliminate some of the undesired modes and did have a resonance which corresponded to a longitudinal mode. However this probe could only handle twice as much power as the transmitter probe. The cutting action of this probe was also evaluated on an empty pad and none was observed. The further refinement of these "power" probes was therefore unwarranted and was discontinued.

At this point a slightly different approach was taken. Since two longitudinal probes had been constructed and tested for transmitters, it was decided to use one in the risk assessment. In this case either the probe, solder joint or IC could fail. If the transmitter failed first then there would be no chance to fail the circuit.

The quad nand gates were used again for this study. The receiver and transmitter were placed on the solder joint in the normal inspection position. The two spectra shown in Figure 21a were taken with the HP 3585A. These were the received spectra obtained when the transmitter was operated over the range of the tracking generator output. The lower trace corresponds to a peak-to-peak voltage across the transmitter of 0.35 volts. The upper trace corresponds to

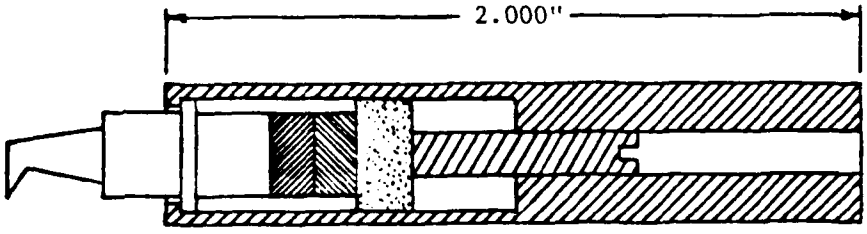

FIGURE 19a. DESIGN OF "POWER" PROBE NO. 1

[The small cross-hatched areas on the axis of the probe are the PZT-4 elements and the speckled area is damping material.]

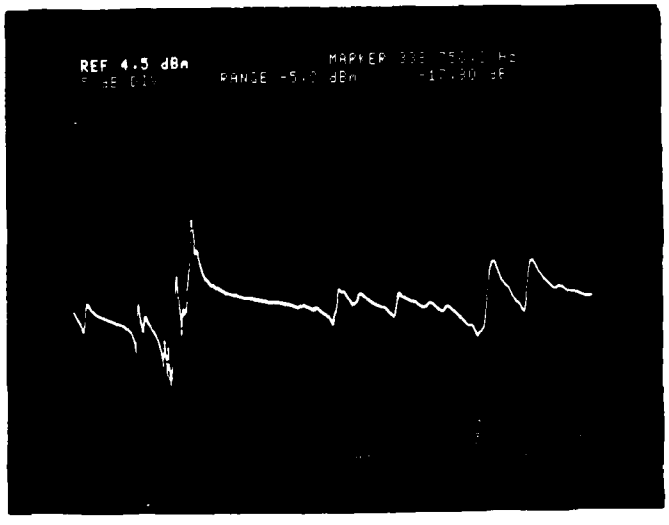

FIGURE 19b. IMPEDANCE DIAGRAM ($|Z|$ versus f) OF "POWER" PROBE NO. 1

[While many relatively large resonances are apparent, none of these were the desired longitudinal mode.]

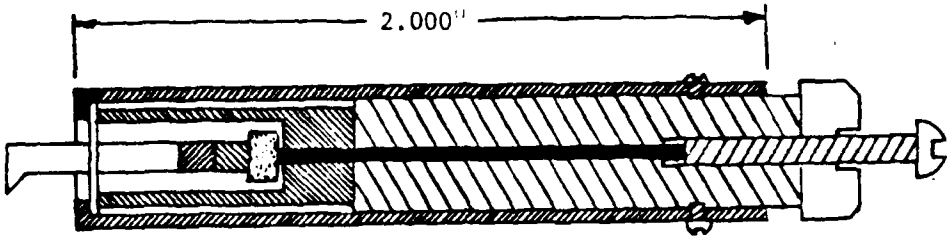

FIGURE 20a. DESIGN OF "POWER" PROBE NO. 2

[The small cross-hatched area on the axis of the probe are the PZT-4 elements and the speckled area is damping material.]

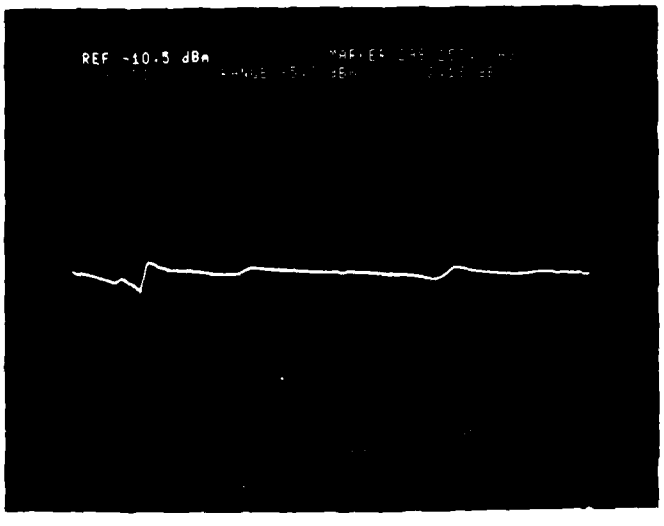

FIGURE 20b. IMPEDANCE DIAGRAM ($|Z|$ versus f) OF "POWER" PROBE NO. 2

[Note resonance at 298.5 kHz is the designed longitudinal mode.]

a peak-to-peak voltage across the transmitter of 1.35 volts. An ENI 240L Class A power amplifier (50 dB gain) was inserted between the tracking generator and the transmitter. The maximum limit of the input to the power amplifier is exceeded when the tracking generator output is at its maximum. Therefore the output was set in its midrange. The measured peak-to-peak voltage drop corresponded to about 120 volts which is two orders of magnitude (51, 39 dB respectively) greater signal than the normal signalling levels. A received spectrum at this signalling level which is shown in Figure 21b was obtained from the same joints as before. It is interesting to note that the spectral shape does not change significantly and that the received signal increased in proportion to the increase in the drive signal to the transmitter. This implies that the transmitter, joint and receiver act as a linear system over this frequency range and power level.

Each joint of an IC was inspected for 30 seconds at this increased level. The 30 seconds is an inspection time roughly at 100 times greater than is typically used. After all 14 leads of the IC were inspected the performance of the IC was checked. All of the four nand gates operated properly and no visual damage to the leads could be observed. At this point, the IC was going to be retested at the same power level but for a duration of a minute for each joint. Two joints were tested when the power amplifier failed. The functionality of the IC was checked and was again found to be working properly. The risk assessment tests were suspended at this time.

Therefore even after the joints of an IC were inspected at signal levels at 100 times greater than normal and for durations also 100 times greater than normal, no damage to the transmitter, joint, IC and receiver was observed. These tests are not definitive and could be extended to longer times and power levels. However, they do indicate a large safety factor for normal inspection.

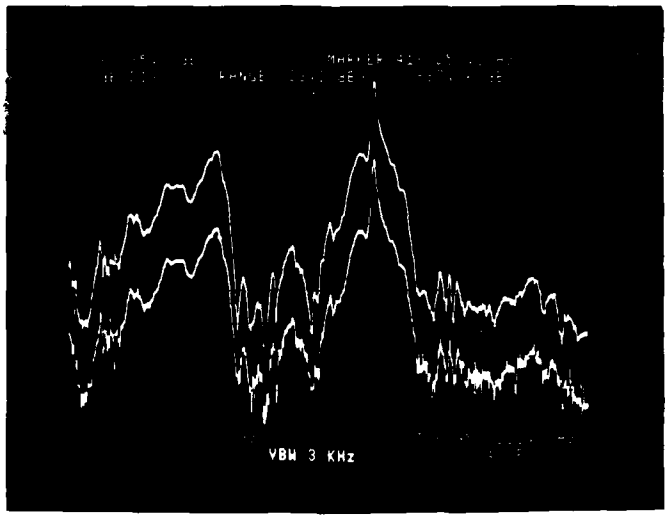

FIGURE 21a. SPECTRAL RESPONSES OF THE RECEIVED SIGNAL THROUGH A JOINT OF THE IC #MC2101F

[The top curve was obtained when the signal to the transmitter was operated at the maximum output of the tracking generator of the HP3585A Spectrum Analyzer. The bottom curve was obtained with the minimum output of the tracking generator. This is the range that is used when inspecting joints.]

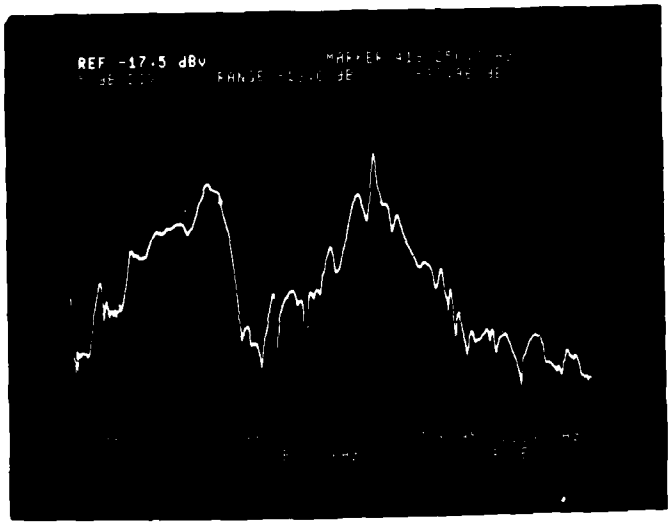

FIGURE 21b. RECEIVED SPECTRUM WHEN SIGNAL STRENGTH TO THE TRANSMITTER IS ROUGHLY 100 TIMES GREATER THAN USED DURING NORMAL INSPECTIONS

[Note difference in reference levels (REF) in Figures 21a and 21b.]

CONCLUSIONS

It may be concluded that probe assemblies of the type designed and used during this contract period used in conjunction with simple algorithms developed during this contract period can on the basis of computer-generated decisions distinguish experimentally prepared good lap solder joints on ribbon leads from similarly prepared joints having heel cracks with a high degree of accuracy. Decision making speed of the system with which these experiments were done was slow. However that deficiency will be overcome in dedictated instrumentation.

It is concluded that the ultrasonic technique as presently employed can distinguish good from cracked joints in round leads with a moderate degree of success. It seems reasonable to anticipate that the system may be refined to accommodate lap joints of differing conformations.

With respect to defect types in lap solder joints other than heel cracks, a clear delineation of possibilities cannot be made at this point.

Finally, it may be concluded that the risk of damaging the articles under inspection with the ultrasonic energy used for that inspection is very remote.

ATTACHMENT 1

DISTRIBUTION LIST

ATTACHMENT 1

DISTRIBUTION LIST

Warner Robins Air Logistics Center/PPWVA (1tr only)
Director of Procurement and Production
Attn: Mr. John H. Blair, Contracting Officer
Robins Air Force Base, Georgia 31908

DCASMA, Dayton (1tr only)
Attn: Mr. Larry Connaghan, DCRO-GDCA
Administrative Contracting Officer
% Defense Electronics Supply Center
Dayton, Ohio 45444

Vanzetti Infrared and Computer Systems, Inc. (1)
Attn: Dr. Alan Traub
Advanced Development Manager
607 Neponset Street
Canton, Massachusetts 02021

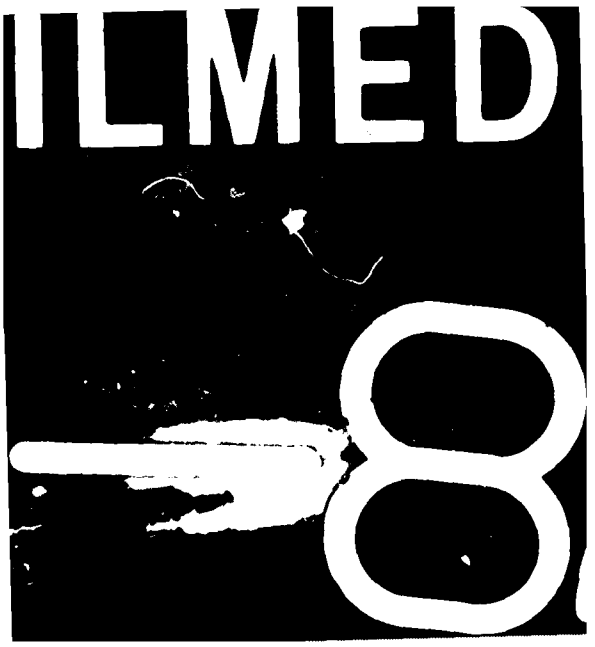
ILMED
8